MASTER OF PHILOSOPHY

Highly tunable room temperature quantum cascade lasers

Mackenzie, Fardeen Fraser

Award date:
2011

Awarding institution:
University of Dundee

MASTER OF PHILOSOPHY

Highly tunable room temperature quantum cascade lasers

Fardeen Fraser Mackenzie

2011

University of Dundee

Highly Tunable Room Temperature Quantum Cascade Lasers

Fardeen Fraser Mackenzie

A Thesis presented for the degree of
Master of Philosophy

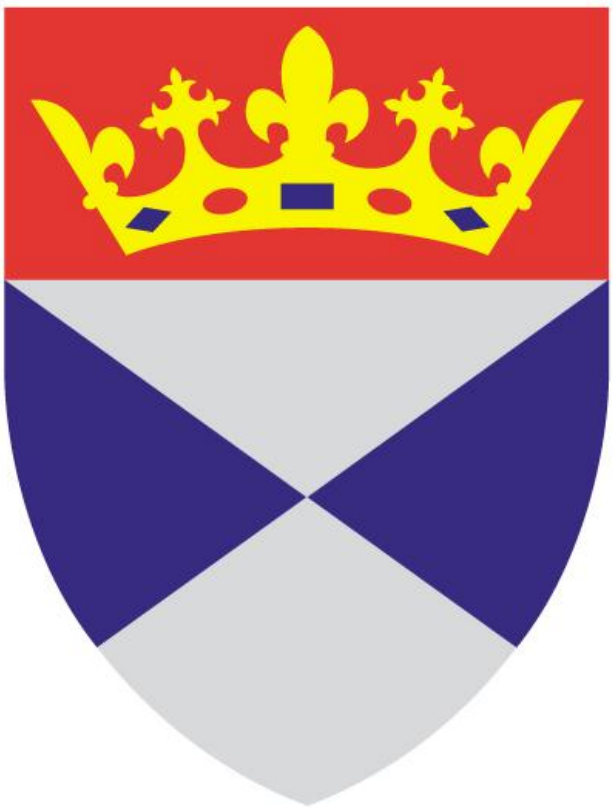

Photonics and Nanoscience Group
Department of Electronics and Physical Sciences
University of Dundee
UK

July 2011

Acknowledgements

I'd like to extend my utmost thanks to my academic supervisors namely Edik Rafailov, Natasha Bazieva and Suydulla Persheyev; without their constant support, patience and encouragement throughout the past two years this project could never have been possible. I'd also like to thank our industrial partner M-Squared lasers particularly Graeme Malcolm and David Jackson, their continued faith and belief in the project helped to push progress even through the rough patches that all projects are subject to.

Declaration

I, Fardeen Fraser Mackenzie, hereby certify that this thesis has been written by me, is a record of work carried out by me, that it has not been submitted in any previous application for a higher degree and that unless otherwise stated, all references cited have been consulted by me.

Signature Date

Abstract

An investigation was conducted into the feasibility of novel Quantum Cascade Laser technology to replace Optical Parametric Oscillator based light sources in real-time video-rate gas imaging systems. A number of required features were defined and verified by laboratory experimentation showing that the novel QCL technology is a good candidate to replace OPO based devices.

Table of Contents

Table of Figures

Thesis Synopsis

This thesis contains a record of an investigation conducted to determine if novel Quantum Cascade Laser technology might be used as a light source for real-time video-rate gas imaging devices.

The thesis is segmented into three sections; the introduction section acts as a brief review of the state of QCL technology and charts the development history if these devices and their antecedents. The second section is mainly concerned with the real-time video-rate gas imaging, its importance in industry and science as well as current technological solutions. Also covered in this section will be the reasons why a QCL light source might offer several advantages over current solutions. Finally the last section will describe the experiments which were designed and conducted in order to determine if the new QCL technology is indeed a viable source and a conclusion made based on the results of these experiments.

Introduction

Technological Background and History

Lasers

Light Amplification by Stimulated Emission of Radiation conceptual groundwork was first laid out in the eminent scientist Albert Einstein's 1917 paper Zur Quantentheorie der Strahlung (On the Quantum Theory of Radiation). In his paper Einstein re-derived Max Planck's law of radiation based upon probability coefficients for the absorption, spontaneous emission, and stimulated emission of electromagnetic radiation. As with many of Einstein's theories it was not validated until a number of years later in 1928 when Rudolf W. Ladenburg observed both stimulated emission and negative absorption (1). By 1939 Valentin A. Fabrikant had predicted the use of stimulated emission to effectively amplify short waves and in 1947 Willis E. Lamb and R. C. Retherford were the first to exhibit stimulated emission.

The first MASER was demonstrated by Charles Hard Townes in 1953 (1). Townes' contemporaries working within the Soviet Union Nikolay Basov and Aleksandr Prokhorov were simultaneously working with quantum oscillators and produced a system which incorporated gain media which more easily achieved population inversion by containing a third energy level – thereby allowing emission to occur between an excited state and lower state rather than the ground state and so being capable of continuous emission. These achievements contributed to all three men being awarded the Nobel Prize in Physics in 1964.

A few years after demonstrating a working maser Townes and a colleague at Bell labs, A. L. Schamlow began working on a similar device that would produce light in the visual spectrum, the so called 'optical maser'. By 1957 Gordon Gould had coined the term LASER and had documented the idea of using an open resonator at around the same time as Prokhorov published the same idea in the USSR. In 1959 Gould published the first paper to contain the term laser (2).

Eventually it was Theodore H. Maiman who on 16th May 1960 demonstrated the first functioning laser. This first example was based on a ruby crystal pumped by a flashlamp and operated at 694nm though it was only capable of operating in a pulsed mode. This point marked the explosion in laser science and soon far superior lasers were designed, within the year Maiman's ruby laser was made obsolete when Ali Javan et al. built the first gas laser based on helium and neon which operated continuously in the infrared (3).

However public and general opinion of these new discoveries was low, despite Gould's paper where he listed a number of possible applications for the laser it was largely considered a scientific curiosity, a so called 'solution looking for a problem'. This seems ironic in the modern age as lasers have permeated virtually every facet of life, from entertainment to engineering, communication to medicine, construction to security - lasers now push these fields ahead as they are continuously improved and enhanced.

Diode Lasers

The diversification of lasers was almost immediate, now there are many types of lasers generally classified by their gain medium these include gas lasers, chemical lasers, excimer lasers, solid state lasers, free electron lasers and recently even bio lasers (4) (5) as well as many others, each of these lasers generally has many sub categories as well.

One of the earliest predicted types of lasers and subsequently most prolific is the semiconductor laser. Also known as laser diodes, semiconductor based lasers use a semiconductor material as the gain medium and generally rely on electrical pumping to achieve population inversion and lasing though optically pumped laser diodes also exist. The key difference between laser diodes and most other types of lasers such as gas lasers is their size; diode lasers by comparison are extremely small and compact as well as benefiting from a very well established scientific and manufacturing background. Generally this makes them exceedingly cheap and reliable.

There are a number of different types of laser diode; one of the simplest is a double heterostructure laser which essentially consists of a layer of low band gap material wedged between two higher band gap layers. The classic materials used are gallium arsenide and aluminium gallium arsenide. If the middle layer can be made thin enough it will effectively quantize the variation of the electron's wavefunction and thus the component of its energy; this makes the diode a quantum well laser. Quantum well lasers benefit from higher efficiency than ordinary double heterostructure diodes due to the fact that the density of state of electrons within the well have an abrupt edge – this concentrates the electrons which are in energy state conducive to lasing. Quantum Well lasers vary in design and include those with multiple quantum wells or even quantum 'wires'. One of the most important variations comes from a multiple well design where the difference between the well energy levels is used as the lasing transition rather than the bandgap. This type of laser is known as a Quantum Cascade Laser.

Quantum Cascade Lasers

Currently Quantum Cascade Lasers can emit light in regions of the electromagnetic spectrum such as THz and the mid- to far-infrared region. They are a relatively recent invention despite being predicted by Kazarinov and Suris in 1971 (6), the first QCL was only demonstrated by Federico Capasso et al at Bell Laboratories in 1994 (7).

Whereas in traditional bulk semiconductor crystal electrons may only occupy two states in either the conduction band or the valence band (emitting a photon during the transition from the former to the latter) with the wavelength of the emitted photon being dictated by the band gap of the material system, QCLs are comprised of a superlattice of many layers of differing materials. This superlattice provides a varying electrical potential across the length of the device, therefore the probability of an electron inhabiting a position changes along the device. As a result the permitted energy bands are split into a number of discrete sub-bands; this is known as one-dimensional multiple quantum well confinement. Well-designed systems can be made to achieve population

inversion between two sub-bands and therefore create laser emission. One important difference between a QCL and other devices is self-evident from their construction – the wavelength of emitted light can be tuned to a degree by altering the thicknesses of the material layers without changing the actual material. The other crucial difference is that after 'falling' to the lower energy state and emitting a photon the electron can then 'tunnel' into the next part of the structure and fall yet another energy level emitting yet another photon. This means one electron can provide many photons compared to the standard laser diode model of one electron in one photon out and makes quantum efficiency of better than unity possible and often leads to much higher output power when compared to other types of semiconductor based laser diodes. In figure 1 a population inversion must exist between state 3 and state 2, this is facilitated by state 1 being only one optical phonon energy (~34meV) below state 2 and thus a very fast relaxation time of around 0.1-0.2ps exists in comparison to the relatively long lifetime experienced in state 3.

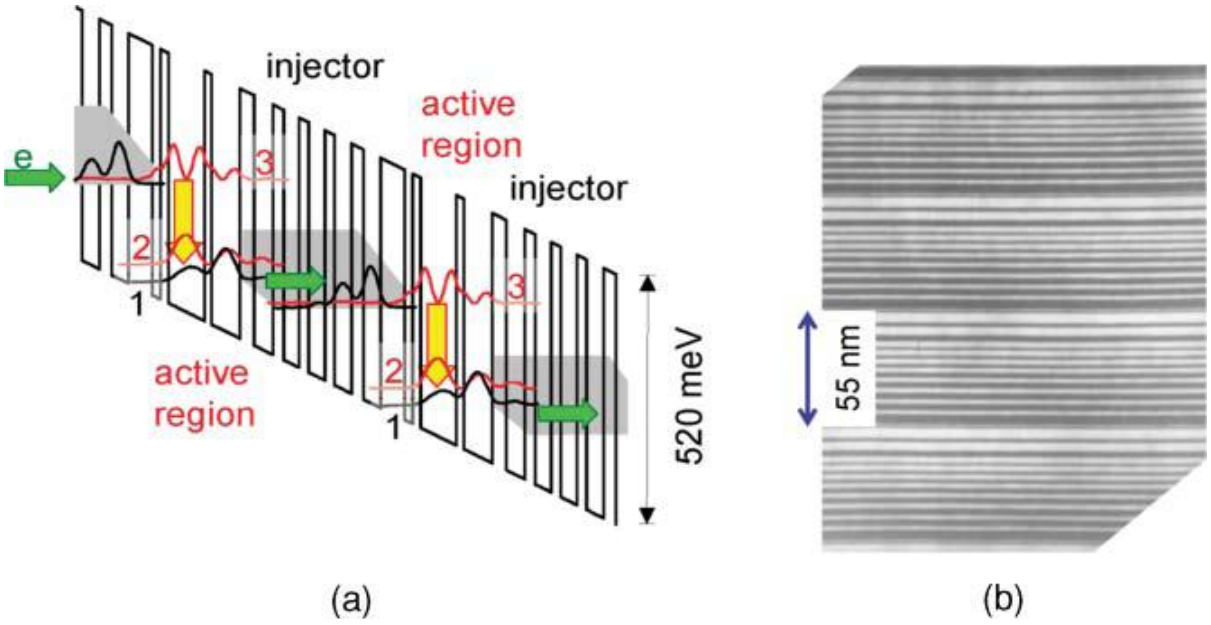

Figure 1. (a) Energy diagram of a quantum cascade laser emitting at λ = 7.5 μm. Each stage (injector plus active region) is 55 nm thick as shown in (b) which shows a transmission electron microscope picture of a portion of the structure. The white and black contrast regions represent the well and barriers, respectively (8).

Optical Waveguides

Like most diode lasers QCLs require a feature which confines the gain medium into an area of desired shape and size in order to make it easy to direct the collimated light and allow a resonator to

be coupled so that feedback is achieved. There are a number of commonly used optical waveguides in QCL fabrication, one of the simplest is a ridge guide. A ridge waveguide is very simply created by etching two parallel trenches on either side of a strip of gain medium. Width and length vary but generally widths are < 12µm, length is generally in millimetres. A dielectric material will be deposited on the trench to guide current into the gain medium, afterwards the entire area is normally coated in Au to act as an electrical contact as well as a heat spreader to help cool the active area.

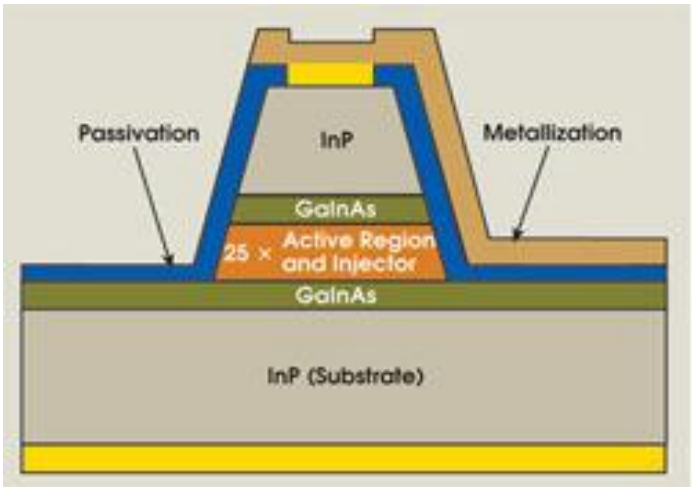

Figure 2. Example of the design of a QCL ridge guide and possible materials on the left (24).

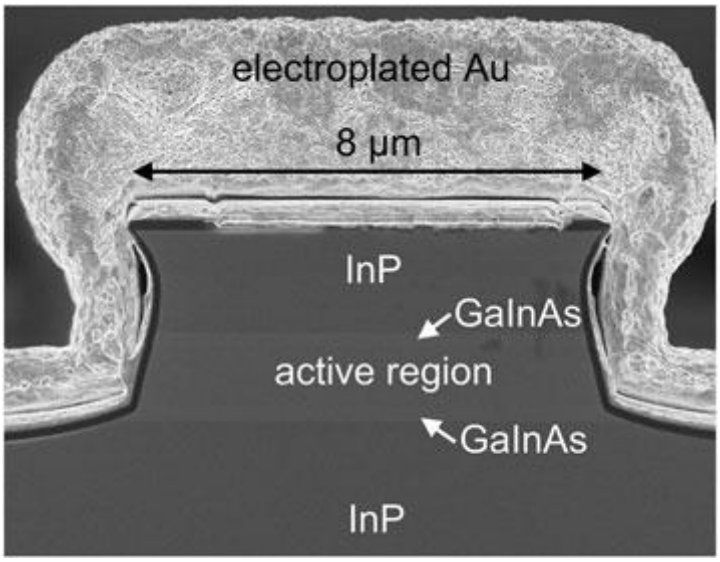

Figure 3. SEM photgraph of a ridge guide QCL (25).

Another very common optical waveguide is known as a buried heterostructure. Like the ridge guide the gain medium is etched to create an isolated ridge, however an additional step is taken where a semiconductor material is then grown over the ridge. The materials will have been selected to

ensure that the refractive index encountered between the two materials is sufficient to act as a waveguide. A dielectric material will also be deposited as in the ridge guide. Heterostructures are generally harder to produce but benefit from removing much more heat from the active area than a normal ridge guide can.

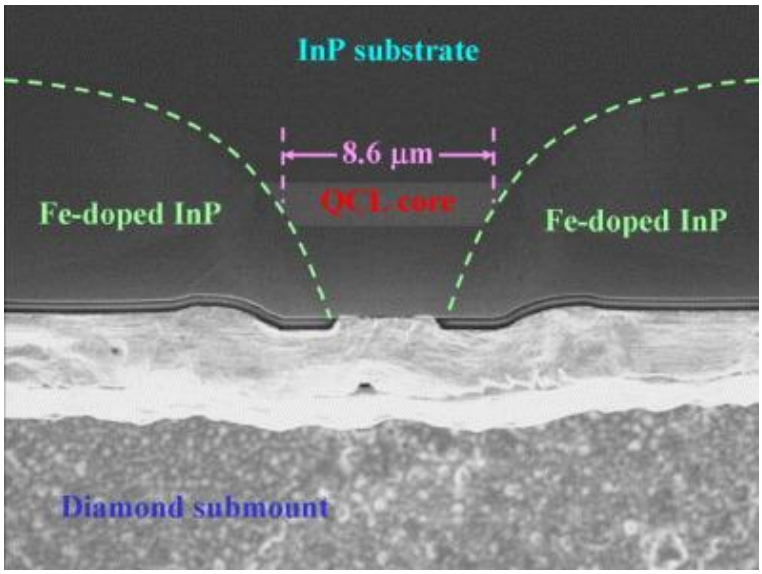

Figure 4. Buried Heterostructure within a QCL (26).

Types of QCL

There are a number of differing types of QCL mainly categorised by their cavity content. A brief summary follows:

Fabry Pérot lasers are one of the most common types of diode laser, consisting of the gain medium etched to create the optical waveguide the two ends of the waveguide are then cleaved in a way that produces two parallel facing mirrors on either side of the waveguide, the reflectivity from the medium/air interface is enough to create a resonator. This is known as the Fabry-Pérot resonator. QCLs based on this design have been shown to produce high power outputs (15) but are often multi-mode as current increases, they also exhibit very poor tunability and what little tuning can be done generally must be conducted by temperature control.

A slightly tweaked version of the Fabry-Pérot involves bonding a distributed Bragg reflector to the top of the waveguide to create distributed feedback; this prevents emission of any other wavelength

or mode other than the desired one. Tunability is still exceedingly poor with these devices and must be conducted thermally although rapidly pulsing a DFB-QCL has been shown to rapidly chirp the wavelength of the laser during the course of the pulse, this has been used to rapidly scan a small spectral region (16).

In an external-cavity set up the QCL acts as a gain medium, usually anti-reflective coating are applied to one or more facets to overcome the reflectivity of the cleaved facets. External devices are then used to create the cavity, there are a number of different designs and set ups for external-cavity the simplest would involve two parallel mirrors facing the facets thereby creating an optical cavity. One of the primary reasons for using an external-cavity set up is its capability to include a diffraction grating which can selectively return precise wavelengths of light depending on its angle to the facet. This effectively means being able to tune the laser output, setups incorporating diffraction gratings have been shown to tune over 15% of a QCL's central linewidth (17). A fuller explanation of external-cavity design and application is covered later in the document.

Applications

The first DFB lasers became commercially available in 2004 (18) followed closely by broadly-tunable external-cavity QCLs in 2006 (19). For the most part QCLs have seen the largest use in applications that involve spectroscopy, particularly where mobility or size is important. Their high output powers, potential for tunability and room temperature range make QCLs particularly useful for these types of applications such as remote gas sensing. They also include the advantages that most diode lasers have over their solid-state counterparts which are their most common competitor in spectroscopic field such as being cheaper to produce by an order of magnitude and being more reliable coming from such a well-established field of semiconductor science and manufacturing technique.

Addressing Shorter Wavelengths and other Material Systems

Capasso's QCL was manufactured using what became the baseline for much QCL fabrication since, InGaAs/InAlAs was lattice matched to an InP substrate (7). Devices based on this design and material

system generally work well at the mid-infrared and have shown high output powers and high wall plug efficiency of ~30% at room temperature even in continuous wave operation (8) (9) (10).

Four years after Capasso's group demonstrated the InGaAs/InAlAs material system Sirtori et al proved that other material systems were possible when they created a QCL based on GaAs/AlGaAs. There are now a great deal of material systems used, generally being designed and chosen for varying performance levels at different wavelengths. Systems are available which work well from the Terahertz region (11) to the near infrared (12).

One of the major issues effecting QCLs has been addressing the shorter wavelengths of the infrared spectrum. Until recently achieving emission at wavelengths < ~4.5µm required liquid nitrogen cooling (13). Shorter wavelengths are determined by quantum well depth, therefore to achieve shorter wavelengths it is necessary to design QCLs with very deep quantum wells. Recent advances in material systems such as InGaAs/AlAsSb and AlInAs/InGaAs has pushed the possible wavelengths to be shorter and shorter; this will be addressed more fully later in the document.

It is also worth noting that the nature of QCLs is such that some materials previously discarded as possessing poor optical qualities may be utilised efficiently in a QCL. For example D. J. Paul has suggested a Si/SiGe silicon based material system (14). This is possible because while an indirect bandgap material like silicon has varying electron/hole energies depending on carrier momentum (carriers change momentum slowly through a scattering process adversely effecting photonic emission), momentum does not affect the intersubband transitions of a QCL.

While there are many material systems and designs of traditional semiconductor lasers in the telecom region it has been a major challenge to achieve similar performance characteristics in the mid-infrared territory as seen in the shorter wavelength region. In particular one of the most useful regions is the so-called molecular fingerprint region (~3µm-20µm), which is enormously useful for trace gas analyses and general spectroscopy, has been hard to address with traditional

semiconductor lasers. One of the main reasons for this has been the reliance on the bandgap to control emitted wavelengths in this region. As we reduce the bandgap the semiconductor laser's operation becomes much more sensitive to operating temperatures – temperature stabilisation, thermal recycling and other mechanisms and phenomena become much more critical to the laser operation. It may also be worth noting that compounding this crucial issue is the fact that with reduced bandgap comes weaker chemical bonds, facilitating manufacturing faults and reducing device reliability (one of the key benefits of using semiconductor lasers). Good examples of this are the common mid-IR semiconductor lasers based on lead salts which exhibit most of these shortcomings (15).

The basic principle of QCLs avoids the bandgap issue entirely as previously explained. However while quantum-well barrier heights are controlled by conduction-band discontinuity for systems generating light > 5µm this is not possible for shorter wavelengths as the upper laser state moves up in energy and so the barrier for thermal energy is reduced. When in operation the active region of these devices can reach temperature tens of degrees kelvin higher than the mount and thus this becomes an extremely limiting factor in terms of operating temperature and optical power. A common method of overcoming this issue is to deepen quantum-wells by strained heterostructures integrating more Al for the barriers and lower In content (AlInAs/GaInAs heterostructures are the most widely reported). Barrier heights of around 0.7-0.8eV are common in these systems which suppresses electron leakage over barriers sufficiently to allow cw operation a little under 5µm (17), as well as extremely high performance - 3W of cw have been reported at 4.7µm (18). Another critical design parameter for thermal performance as reported by Capasso is to ensure that the injector ground state is at least 0.1eV separate from the lower state of the laser transition. If not electrons in the injector can thermally backfill level 2 causing degradation in performance (8). Improved designs utilise a double-phonon-resonance design where three energy levels separated by one phonon energy gap are used to allow larger population inversion and lower thermal backfilling (19).

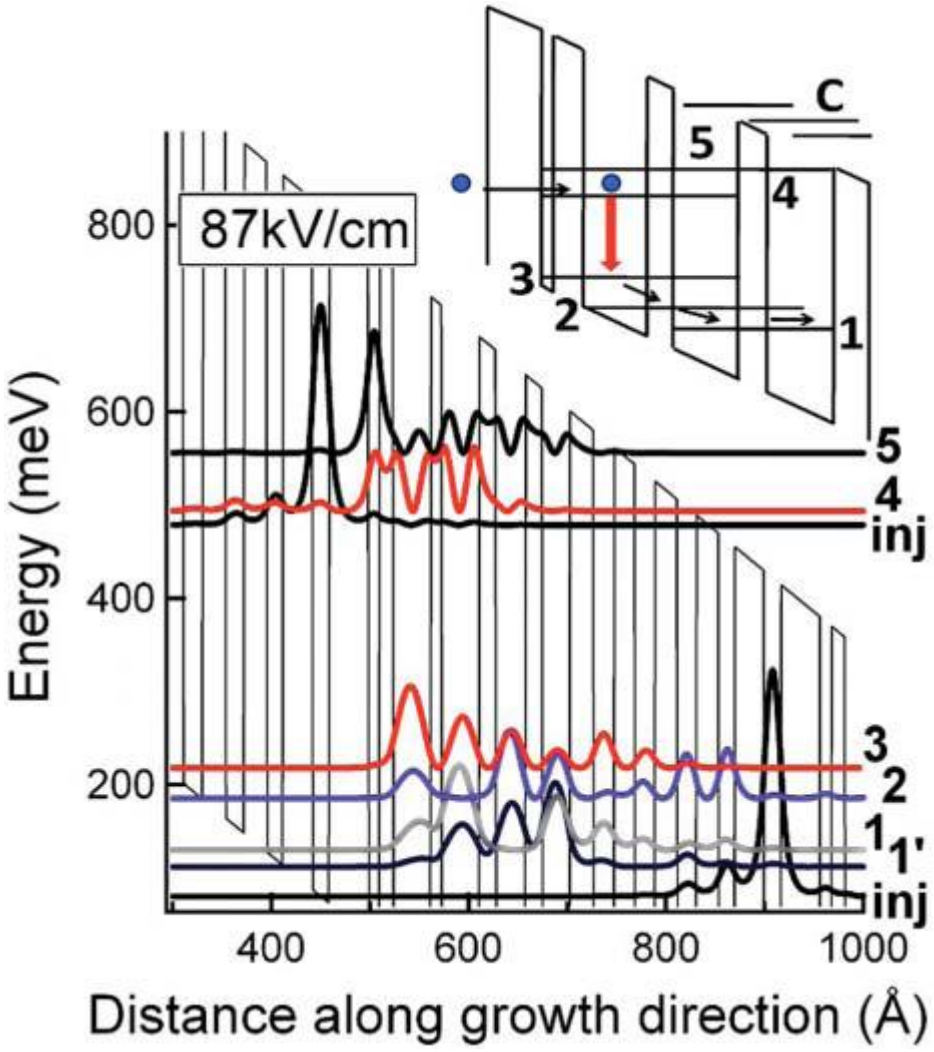

Figure 5. band diagram of a QCL engineered to emit at 4.6µm, inset is an example of a two-phonon-resonant design (8).

Broadband QCLs

Increasing demand from industry and science requires QCLs which are able to be tuned across a wide range of wavelengths. Work has been conducted to integrate arrays of DFB lasers into one unit which is capable of addressing a wide range of useful wavelengths.

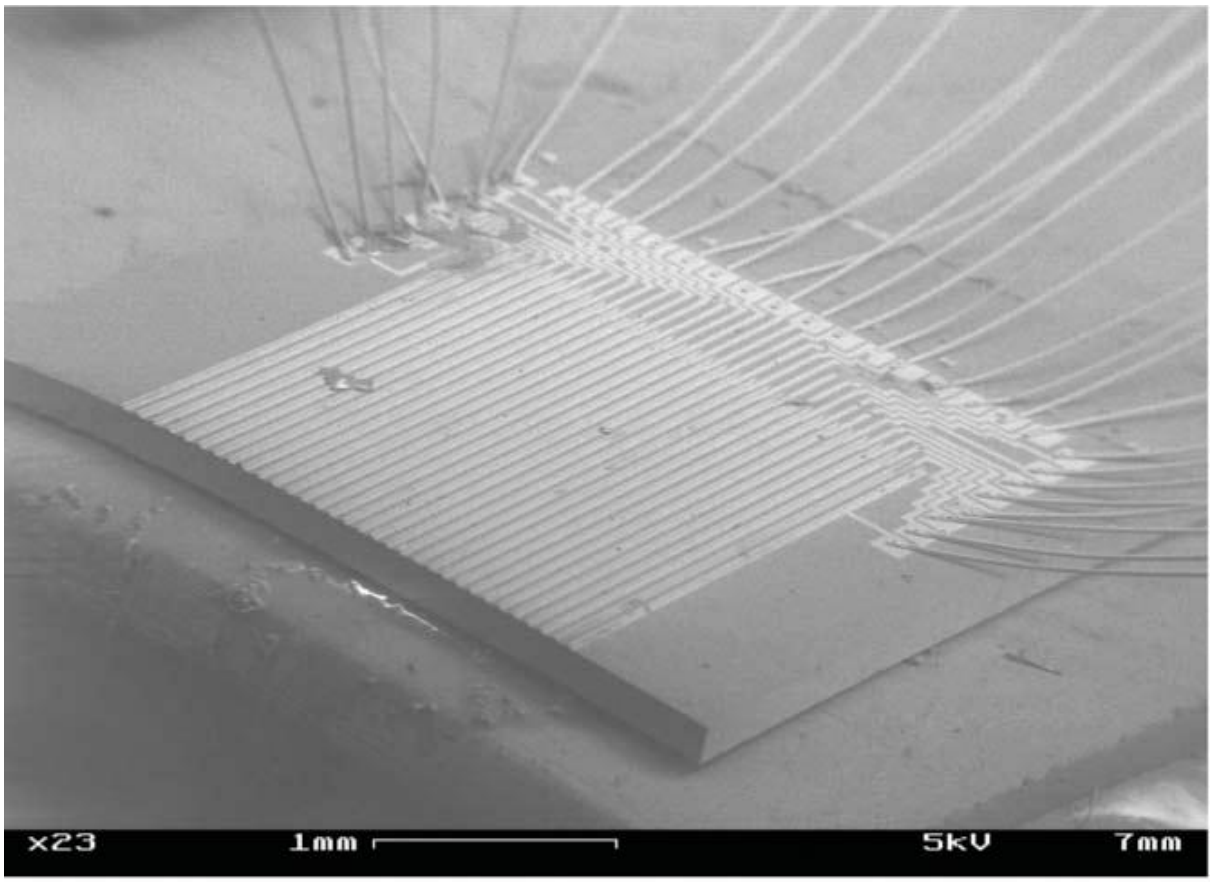

Figure 6. An array of QCL DFB lasers used in a spectrometer (20).

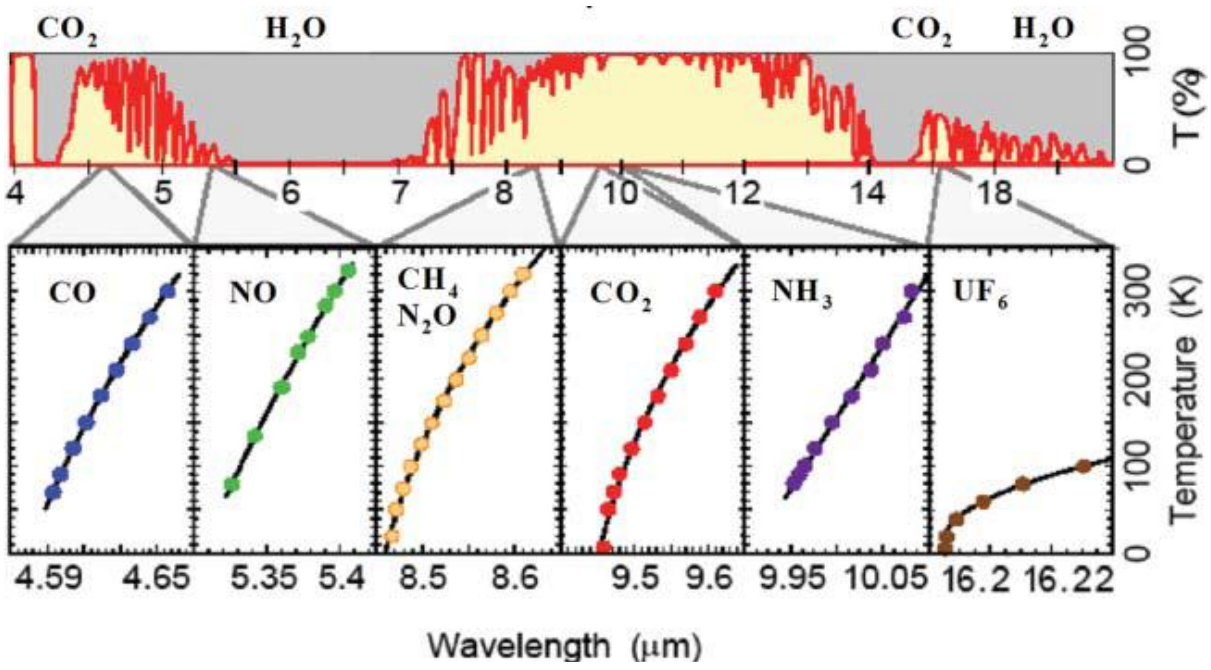

Figure 7. Transmission spectrum under standard conditions for a number of gases of interest. These higher wavelength regions exhibit 'windows' below 5μm and between 8μm and 13μm. Below is shown an array of DFB devices which can be thermally tuned to the selected regions. Adapted from (20).

The other main method of tuning comes from external-cavity set-ups. At longer wavelengths (7.6 to 11.4 µm) impressive tunability of ~40% of the centre wavelength has been achieved with peak powers of 1W at room temperature with Littrow external-cavity designs (21).

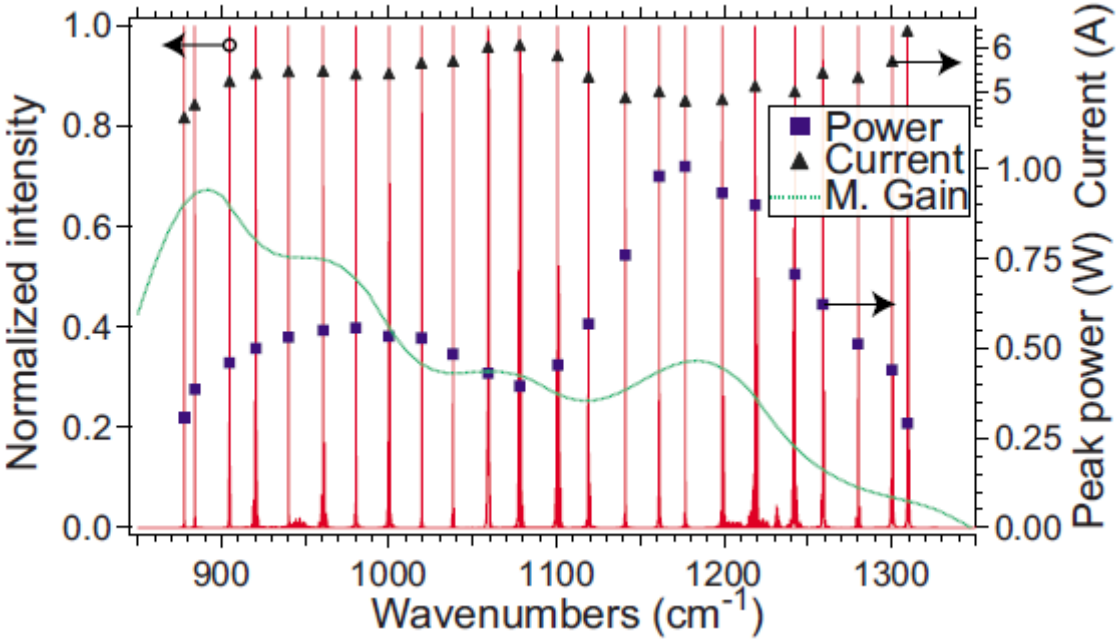

Figure 8. Demonstration of very impressive external-cavity based tuning range (21).

Obviously devices such as these which are able to address the absorption lines of many chemicals are highly desirable. One of the benefits of QCLs over other semiconductor lasers is the ability to design for a quasi-continuum of emission wavelengths by stacking active regions with different central wavelengths.

Figure 9. Example of a multi-cascade QCL with each cascade emitting at a different central wavelength. Such a system can provide a quasi-continuum over which to tune (8).

The ideal situation of course would be to be able to produce a single-mode continuously tuneable broad spectral output. Cutting edge work is focussed intently on this task. The most promising

examples show pulsed QCLs in a Littrow external-cavity set up which achieve single mode tuning from 8.0µm - 9.57µm (22).

QCL Manufacture - Molecular Beam Epitaxy

One of the great benefits of QCLs is that they come from a very well established field of semiconductor science and manufacturing. One of the best established manufacturing techniques is Molecular Beam Epitaxy; this was the method by which our QCL devices were grown.

To be successful MBE is conducted in ultra-high vacuum chambers which allows a very slow deposition rate (< ~1µm/hour) this allows layers to grow epitaxially and offers the opportunity to have very thin QCL layers. Essentially the process involves heating very pure source elements such as gallium and arsenide until it begins to sublimate, the resultant gas is then allowed to condense on the substrate and interact. It is vital for most QCL designs that the layers are precisely the thickness that has been stipulated in the design. Computer control allows chambers within the vacuum chamber which house the different material sources to be closed or exposed to the substrate chamber with such precision that layer growth only 1 atom thick is possible. One of the most common ways used to monitor the layers is Reflection High Energy Electron Diffraction. RHEED acquires information from only the most recently deposited layer. Essentially the system involves an electron gun which fires electron at a known acute angle to the substrate, a detector on the other side of the sample detects some of these electrons and from analysing the diffraction pattern on the sensor a very precise atom specific map can be made of the surface the electrons have contacted.

Real-Time Video-Rate Gas Imaging

Being able to detect the presence and sometimes concentration of a gas is very useful and in many applications is all that is necessary however for many applications this information is simply not enough. Many applications require or would greatly benefit from the ability to visualise the location, movement, size, concentration pattern etc. of the gas cloud/leak etc. One particularly salient sample is within the oil/gas industry where discovering a leak in a pipeline system which covers miles or within a complex system is much faster and can be analysed much more quickly using a video-rate imaging system. Similarly military applications require a very rapid interpretation of laser sourced data, having a video-rate image is ideal for this type of situation.

Our industrial partner M-Squared currently possesses a device which is capable of video-rate imaging of gasses; known as the Firefly-IR the device is capable of pulse repetition rates of up to 150kHz with peak powers reaching 200W. It is used for a number of different applications but most common are spectroscopy, detection of greenhouse gases and hydrocarbons, emissions reduction, mid-IR spectroscopy, oil and gas exploration, medical diagnostics (such as p.p.m. breath monitoring), LIDAR, security and defence (infrared countermeasures, remote detection and imaging of threat agents) and eye-safe illumination. The success of this product and widespread demand from a wide range of industry applications clearly illustrates the need for a device with this wavelength and operating characteristics. However the Firefly-IR suffers from a number of drawbacks. To manufacture the device is rather costly and involves a number of delicate components that require alignment. The mass and dimensions of the device make it unsuitable for most mobile applications or rapid deployment. These issues are symptoms of the core technology used to drive the device; a diode-pumped, intracavity optical parametric oscillator (20).

Optical Parametric Oscillators

The Firefly-IR system is largely based on an OPO system developed by Strothard et al (21), there were many reasons this system was used as the main component of the video-rate imaging device. In the near to mid infrared spectral regions optical parametric oscillators have been shown to very flexible sources of coherent radiation which can be tuned. Although there are examples of OPOs with pulse widths in the femtosecond regime the widest spectral ranges are found in OPOs which operate in continuous wave mode (21). Traditionally systems such as these required very high pump laser powers (~5W) however newer pump-enhanced OPO designs (23) allow the pump wave to resonate within the same cavity as the signal wave and therefore become intensified within the crystal. This system means lower external pump powers are required and therefore allow less powerful and more compact pump sources to be integrated into such systems. Such systems have already been shown to be useful for many spectroscopic applications such as for laser radar (24), molecular spectroscopy (25), photoacoustic spectrometry (26) and trace gas detection (27). In order to achieve good tunability and pulse regimes appropriate for video imaging the Firefly system utilised a cw OPO in tandem with an electro-mechanical polygonal scanner. As previously mentioned while this system provides good laser characteristics it involves many components and mechanical parts which make it delicate, bulky and ultimately very expensive; though much less so than other laser mediums with similar characteristics such as gas lasers. A semiconductor QCL based system would be much smaller, cheaper, involve fewer components, require much less energy as the lasing threshold can be achieved by simple electrical pumping and pulses can be controlled via driving current pulse shaping rather than the electro-mechanical system employed for OPOs.

Novel Quantum Cascade Lasers

As has been discussed and shown achieving lasing at wavelengths of <5µm has proven to be an extreme challenge in the field of QCLs despite high demand for this wavelength region as it houses an atmospheric window and absorption lines of a number of important molecules; particularly methane (CH_4).

Our major collaborators during this project were the University of Sheffield, UK and Montpellier University, France. Montpellier's work with novel materials and band engineering has recently demonstrated pulsed QCLs working at the all-important 3.3µm molecular fingerprint region of methane at room temperatures (40). This is a previously unaddressed region of the electromagnetic spectrum for QCLs except those which were aggressively liquid cooled (41).

Of all the commonly used band structure and material systems InAs/AlSb was selected as having the most potential for short wavelength at room temperature mainly due to the high conduction band offset as previously discussed in this thesis. Montpellier combined this material system and band engineering with a new plasmon-enhanced waveguide which they had initially investigated in 2006 (42) to achieve the short wavelength emission at room temperature.

Statement of Opportunity

As the last section addressed there is a high demand for a tuneable light source at the short wavelength section of the molecular fingerprint region, particularly around the methane absorption point of 3.3µm. Presently the sources used for this task are OPO based and as discussed this renders these solutions as bulky expensive ones. Traditional semiconductor lasers are unable to address this wavelength range; however QCLs have shown some tentative potential to operate at these ranges – though they require aggressive cooling. The recent advances in material systems and band engineering by groups such as those in Sheffield and Montpellier have shown that emission at this wavelength range at room temperature in a pulsed regime is possible with newly designed QCLs. It is from this basic technology that we began to alter designs to develop novel tunability at this wavelength region, as no tunability had been demonstrated at this wavelength region from QCLs before and there is a demand for it from industry and science. We were also keen to ensure the final device would be capable of repetition rates and pulse widths which were capable of video-rate imaging as previously discussed.

Experimentation

High Pulse Frequency Tests

Our investigation began with the very first generation of these novel devices which were Fabry-Pérot units. The size advantage is immediately apparent when compared to OPO based devices which emit at this wavelength.

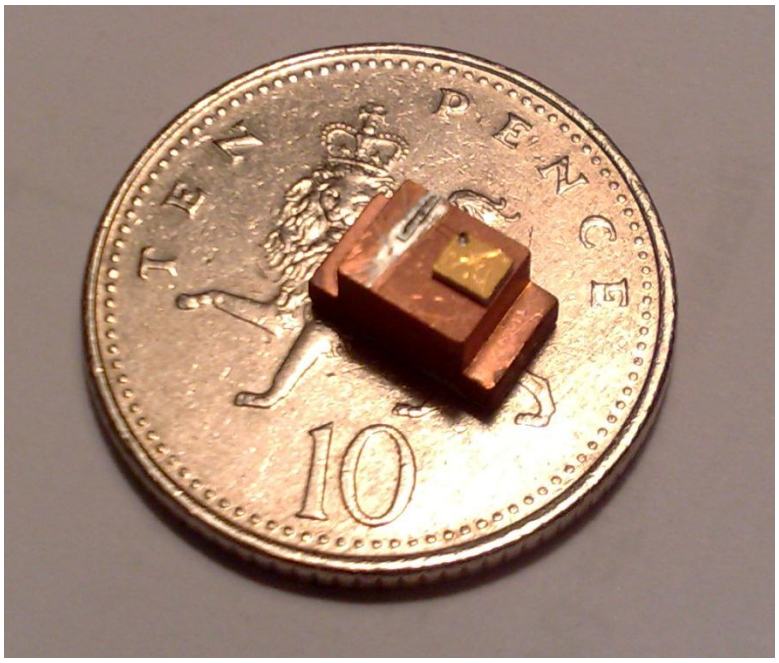

Figure 10. One of the first generation novel QCLs embedded in a copper mount on a UK 10 pence coin for comparison.

The first investigation involved determining if the units would be able to achieve repetition rates that a real-time imaging system would require (>~5kHz), the higher the repetition rate the higher the potential frame-rate of the real time video.

A simple system was built incorporating the QCL mounted on a copper block which was Peltier cooled. A copper wire was bonded onto the top gold mount on the QCL block (the positive terminal) and a second wire bonded to the block itself (the ground terminal). A CaF_2 lens was then aligned at the front facet to focus the light to a broadband power meter. Calcium Flouride lenses were used at this stage due to their commonality and very high transmission (~96%) at this wavelength.

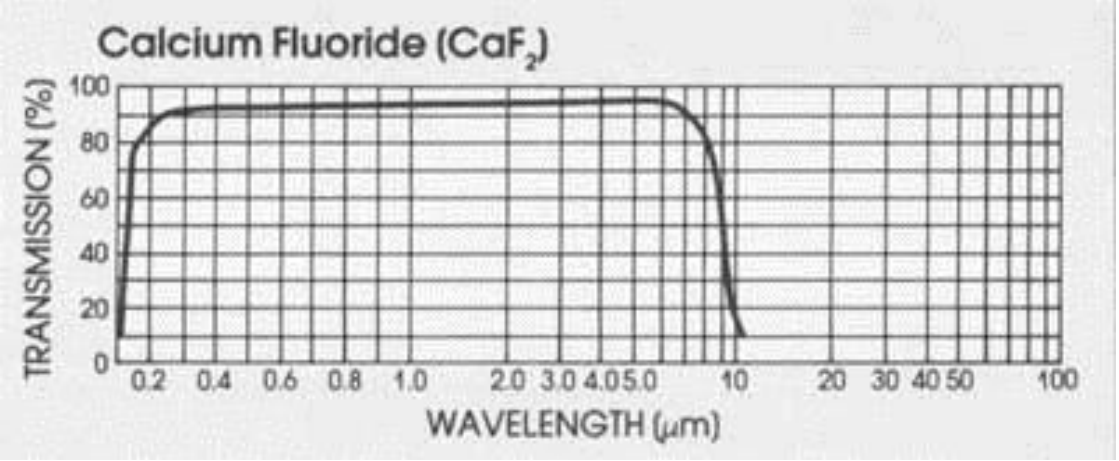

Figure 11. Transmission Spectrum of Calcium Fluoride.

The experiment was conducted in a very low light environment and the power meter was zeroed before the start. The QCL was connected directly to an Agilent Pulse Generator which was capable of producing pulses as low as 5ns with an amplitude of up to 100V/2A.

There was extensive testing with many different pulse regimes. Despite the improvement in terms of effects such as thermal backfilling etc. temperature is still the main concern when running these devices. They also suffer from fairly high localised heat (despite aforementioned improvements), therefore despite Peltier regulation fairly short pulse widths were necessary – generally < 200ns.

Due to the pulsed nature of the device the average power incident on the broadband power meter was very low, in standard expected operating conditions (50ns, 20kHz) too low to register on the meter. However as the repetition rate was increased to higher levels the average power increased to a point where it was easily detectable and better lens alignment was possible.

The Fabry-Pérot devices were found to have very good reliability and high-rep rate operation showed exceedingly high rep-rates were safely achievable at the cost of peak power. This was an early win for the project, though repetition rates this high are not useful for the intended application and impinge on the peak power this is useful knowledge for other applications. The maximum repetition rate without causing rapid degradation was found to be 680kHz (more than enough for video rate imaging), at 700kHz and above thermal issues cased a massive decrease in performance.

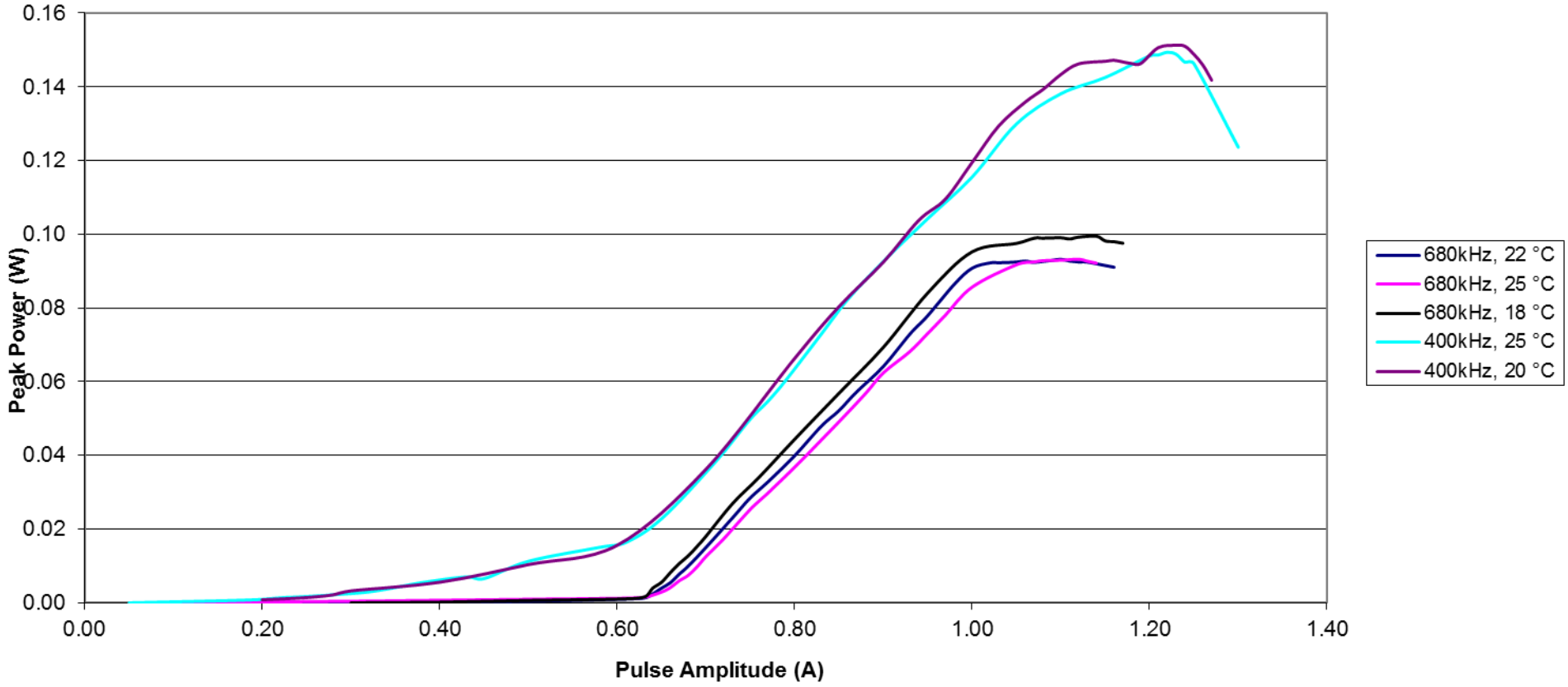

Figure 12. Showing the effect of repetition rate and Peltier temperature on peak power output of a Fabry-Pérot QCL.

Figure 12 shows one sample at a range of repetition rates and Peltier temperatures. Lower temperatures generally yield higher peak powers, this is as predicted however the effect is only slight as the Peltier cooling cannot wholly deal with the very localised heating experienced by the unit. There are also a number of thermal junctions within this set-up which affect the efficiency of the cooling. A greater effect on peak power can be seen by the difference in repetition rate, in this example the higher repetition rates are ~70% higher than the lower ones and show ~50% less peak power. It is predicted that this is mainly due to thermal effects however an investigation into this area is outside the scope of this investigation. The purpose of these tests was to determine if repetition rates of sufficient frequency for video-rate imaging were possible and the result was a resolute positive.

Fabry-Pérot Spectral Output

These samples showed high potential for video-rate pulse frequencies, however as yet their precise wavelength emission was not known. An investigation commenced into determining the operating wavelength for these devices.

The set-up involved the same QCL and mount system with a CaF_2 lens mounted at the front facet. The QCL was connected to the same Agilent pulse generator and the light directed through a ½ meter monochromator. At the exit slit of the monochromator a photodiode was mounted to detect any light which passed through the monochromator. The monochromator consisted of a number of internal gratings and mirrors in a closed system, by adjusting the diffraction grating angles light of a very specific wavelength can be directed out through the exit slit. A PbSe photodiode was selected for its good spectral response in this region.

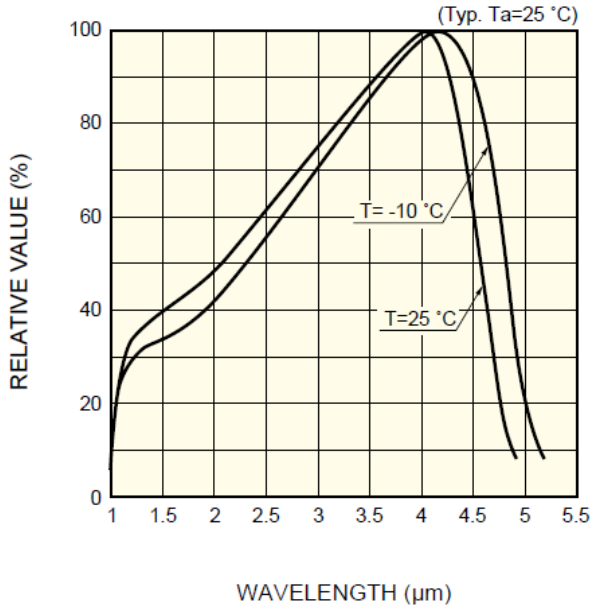

Figure 13. Spectral response of the PbSe photodiode (43).

A custom piece of software was then written to control the gratings and their angles as well as the slight widths etc. in the monochromator (please see the software appendix for more information on this program). The program was then set to adjust the internal gratings to a starting angle at one end of the intended spectral analyses, light was then allowed to flow through the system and the photodiode reading recorded. The angle was then altered very slightly to allow a slightly longer wavelength of light through the system and the process repeated until the predefined end angle was reached. At the end of this process the relative amount of light incident on the photodiode at each of these angles was compiled into one datafile and then analysed and a plot drawn from it. The power is given in arbitrary units and the grating angles have been converted into the corresponding wavelength of light.

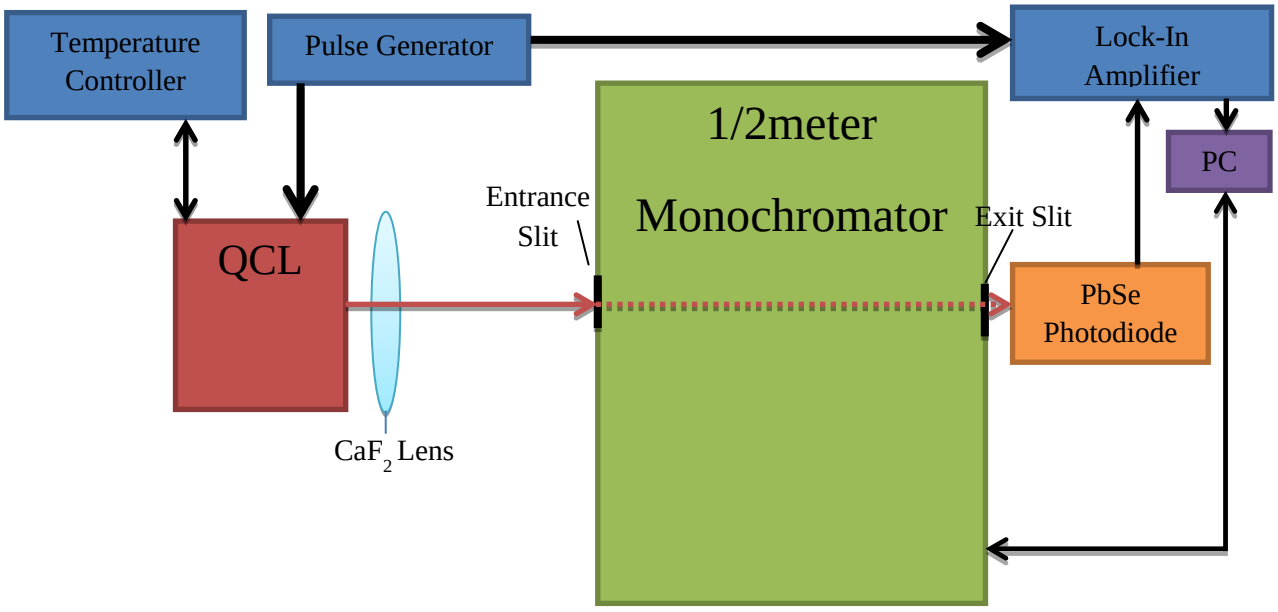

Figure 14. Showing the main equipment involved in the spectroscopic analysis.

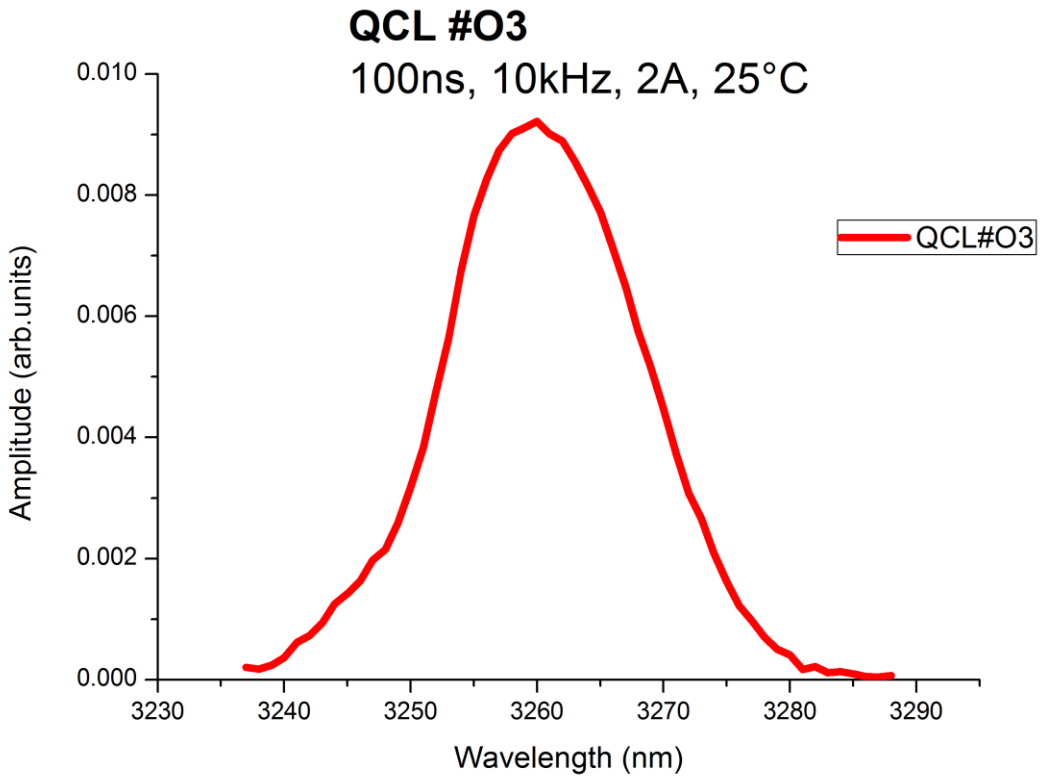

Figure 15. Showing the spectral output of one of the QCLs.

Figure 15 shows that the device is working exactly at the wavelength range we desire 3260nm, it also shows that the device can produce this wavelength range at room temperature easily.

These devices therefore show good potential as possible light sources for the application we are investigating. However thermal tuning of the Fabry-Pérot devices was very limited – again it is assumed that the Peltier thermal control is insufficient to overcome localised heating effects. While it is likely that other thermal control solutions would be effective the application field we are attempting to address can only utilise passive cooling and Peltier systems so other thermal control systems were not investigated as part of this investigation.

Power Delivery Challenges

Soon after the conclusion of the previously described experiments rapid performance degradation of the samples was observed. The samples were rendered in an inoperable state with no evidence as to the reason. The first tests conducted to analyse this problem were to check the IV curves of the devices against those curves that were taken when they were first acquired and tested. To achieve this the samples were mounted in a specialised Keithley semiconductor analyses platform.

(a) (b)

Figure 16. (a) shows the computer control module for the Keithley Semiconductor Characterisation device. (b) shows part of the probe assembly where the QCL is mounted and the probes connected to the sample.

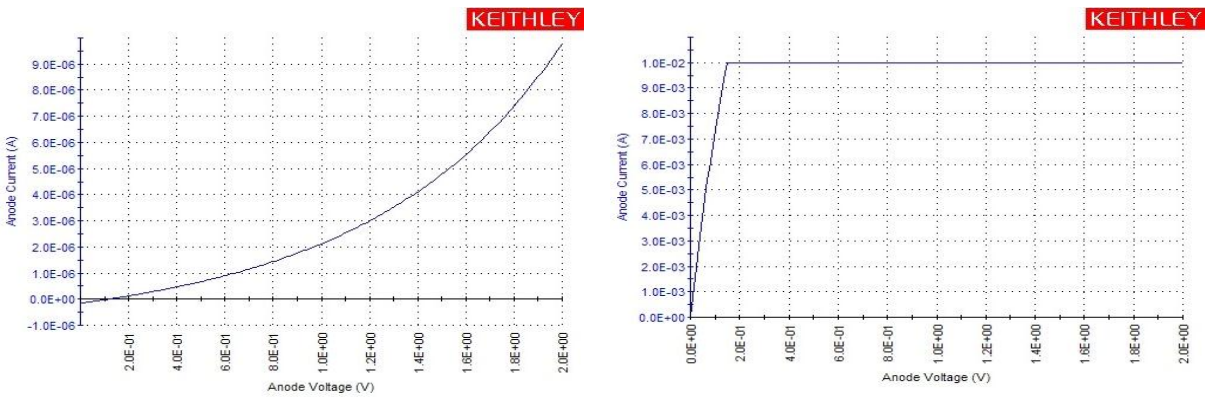

(a) (b)

Figure 17. (a) showing initial IV curves and (b) showing IV curves after testing.

As the IV curves in figure 17 show the samples were no longer functional as diodes and were no longer useful. All the initial samples were found to be in a similar state. A number of hypotheses were formed and tested as to why this may have occurred, if new samples were grown and the same conditions which damaged the first batch were repeated this would severely hamper the investigation.

Eventually testing showed that the electrical pulses produced by the pulse generator were not appropriate for the samples we were investigating. The main issue centred on the internal generator design which forced a 100V bias across the samples which were designed for only around 8V. This issue was unavoidable with this particular generator.

This was only one issue encountered with the power delivery system, as we had the opportunity to have new samples grown we made a move towards designs which held far greater potential for good tunability, however these new designs would require far higher operating currents than the Agilent pulse generator could produce (details on the new samples will be covered later in this thesis).

It was therefore imperative that a new pulsed diode driver was developed or acquired which would be capable of safely driving our samples. A number of features would be required; a minimum of 50ns clean pulse width would need to be generated, at the same time the pulse amplitude would need to potentially be as high as 6.5A. To achieve this fairly high rise and fall times would be necessary. Additionally there should be a pulse repetition frequency of at least 10kHz. All of these features should also ideally be controllable, for instance a set 50ns driver would not be so useful for doing testing on longer pulse widths later on, rather it should be adjustable.

As there was no commercial solution available at the time we set about designing and constructing our own system. Initial designs were fairly simple in theory and revolved around triggering a commercially available transistor with an external pulse (from the Agilent pulse generator) which

would allow current from an external DC source to flow and be drawn by the QCL. The real challenge came from finding components and a design that could ramp up to the high currents necessary and fall quickly enough to maintain the programmable regimes and not cause damage to the QCL. Of course our design would also allow us to control the pulse frequency and width via the external pulse generator. Current control would be provided by manipulation of the external DC source.

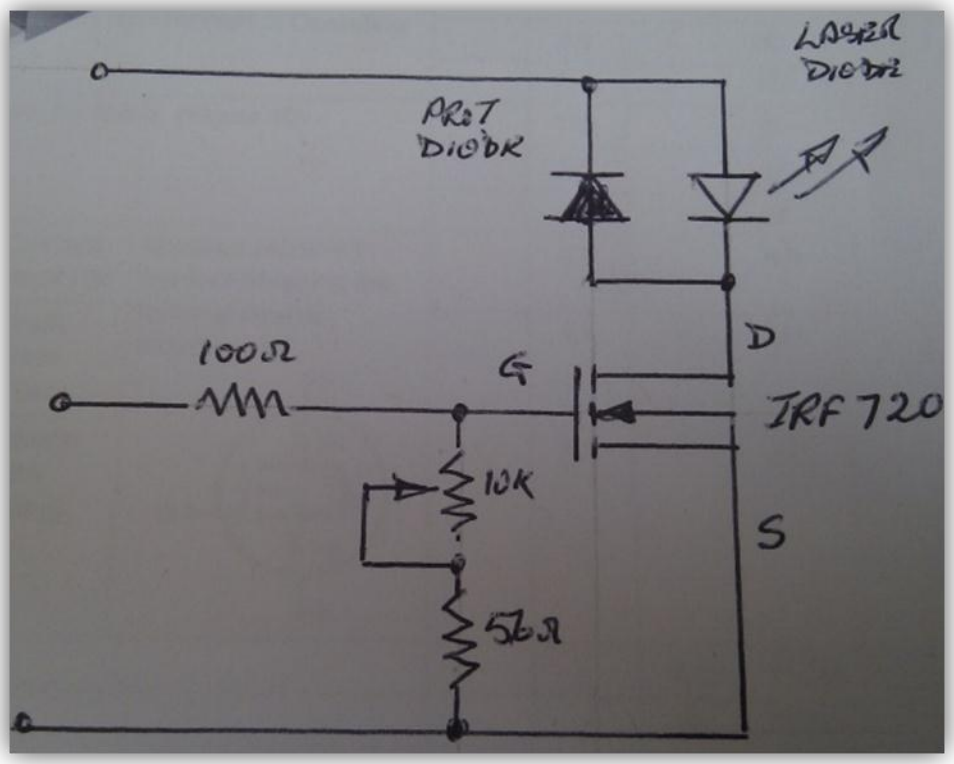

Figure 18. Example of one of the initial circuit designs incorporating a protector diode and an IRF720 transistor.

When deciding on the transistor to use in the design special attention was paid to the maximum current they could handle and their rise and fall times as these were the features most important to allow the fast switching and ramping action that we would require. There were very few options available that could do precisely what we wanted however after accepting some compromises a number of potential transistors were eventually found.

After building a version of the driver it was decided that to accurately test the system without damaging the precious QCL samples that a laser diode driver simulator should be designed and built this would allow the pulses and electrical characteristics of the system to be safely investigated.

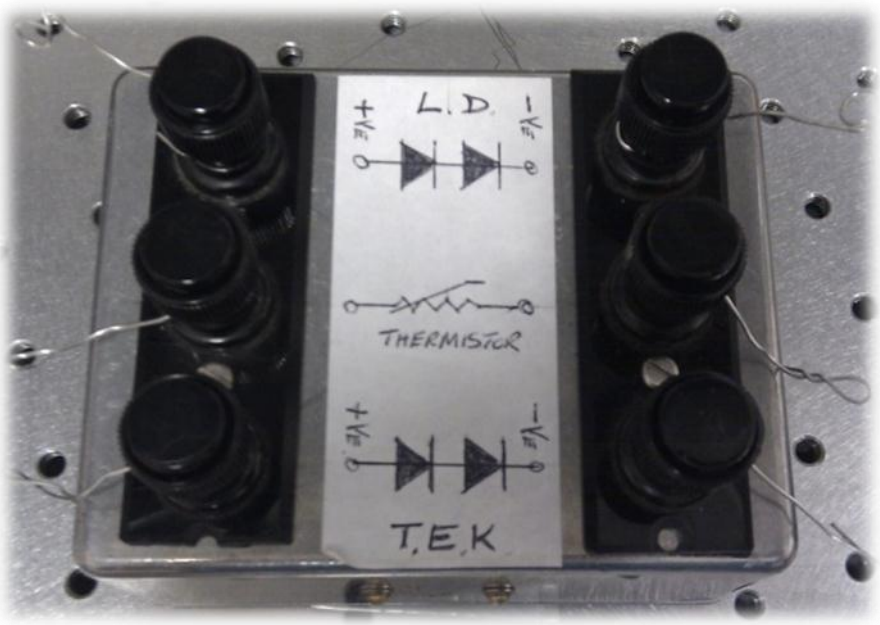

Figure 19. The Laser Diode Simulator test box built to test the pulse driver.

Applying probes to this system and attempting to generate 50ns pulses at 5kHz we observed the pulse shapes generated by the first system.

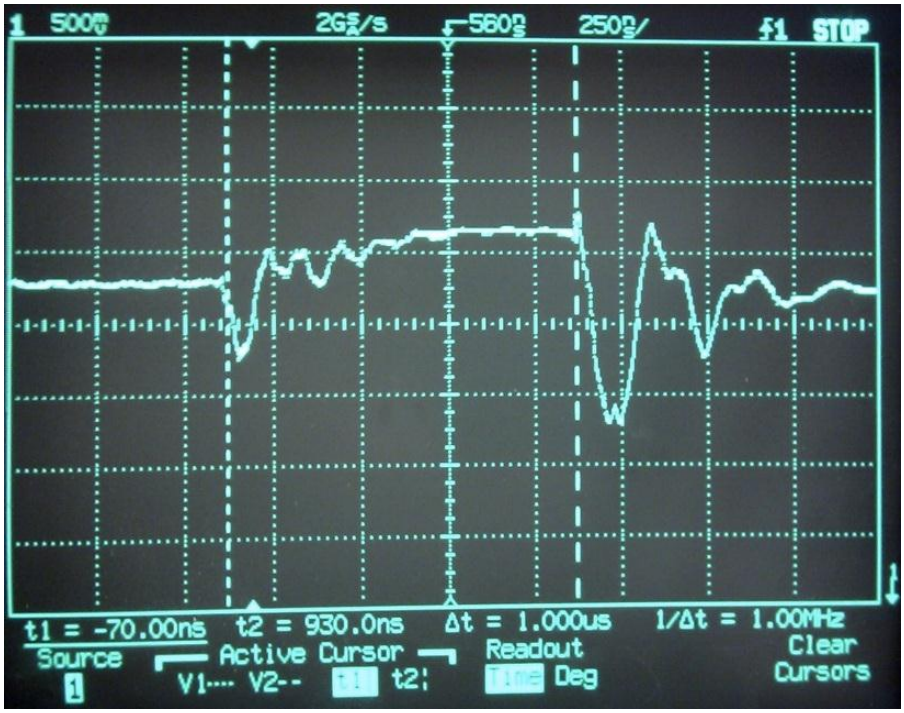

Figure 20. Example of one of the first pulses showing a perturbation of a dc source rather than a true pulse.

Unfortunately the first experiments showed that the system did not work correctly, 'pulses' were generated but these pulses acted as perturbations of the dc source rather than as true sources. In other words as the dc source was increased to 2A the output of the system would be ~2A (minus system losses) with the pulse increasing output minimally for its duration. This was clearly inadequate for our purposes as it would be as if we connected the sample directly to a dc source, this would immediately destroy the device.

A great deal of time was invested in analysis of the internal system, many revisions were made and a number of complete redesigns were necessary. Ultimately the issue we encountered was in unwanted inductance and capacitance within the system which would essentially perpetually saturate the gate and leave the transistor in a permanent 'on' state.

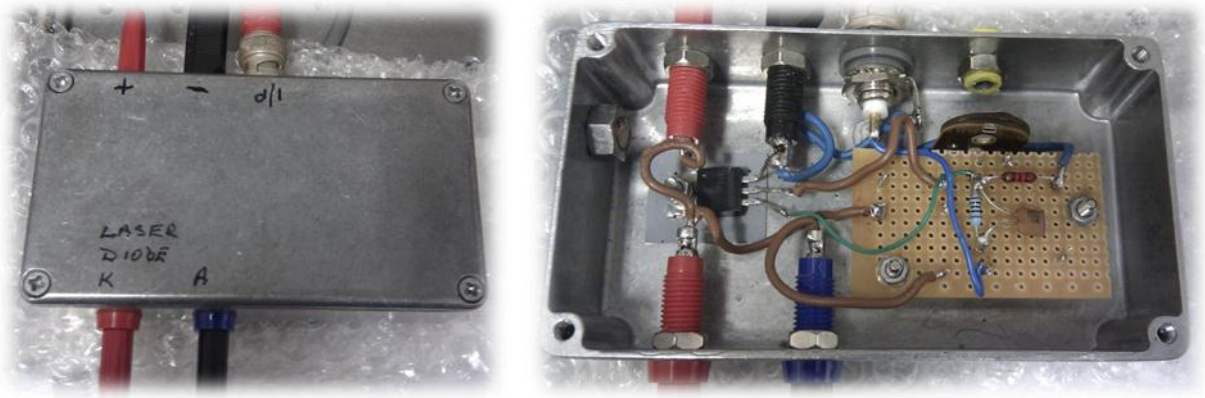

Figure 21. Example of one of the early pulse driver systems custom design and construction. This particular version included a potentiometer which acted as a method to set trigger level for the external pulses. It was though at the time of design that this would help produce better pulses.

Eventually a system was designed which would allow enough time for the problem sections of the circuit to discharge – overcoming the aforementioned electrical effects which were saturating the transistor gate. This lead to a decent pulse shape and a true 'off' state where the QCL would be unable to draw any current except for during the pulses specified by the external generator.

Figure 22. Showing a pulse from one of the 'successful' driver designs.

This final design was found to correctly produce a good pulse with decent shape, unfortunately due to the revision in design which allowed the pulse to be formed the minimum duration of the pulse was increased to ~300ns. Such a long pulse could have detrimental thermal effects on the QCLs,

while it might have been possible to use this system it was decided that it would be more beneficial to continue working towards a system which offered all the features we initially desired.

By this point in development we had found a number of potential commercial OEM solutions that might be able to provide us with the characteristics which we sought. One such device was produced by the Dr. Heller company and would allow us to control the current with the dc source and the pulses with our external generator. One challenge associated with this system was the stipulation that to achieve such rapid rise and fall times the diode could be no further than 6mm away from the output terminals of the device. It was therefore necessary to develop a mounting system that could accommodate this requirement.

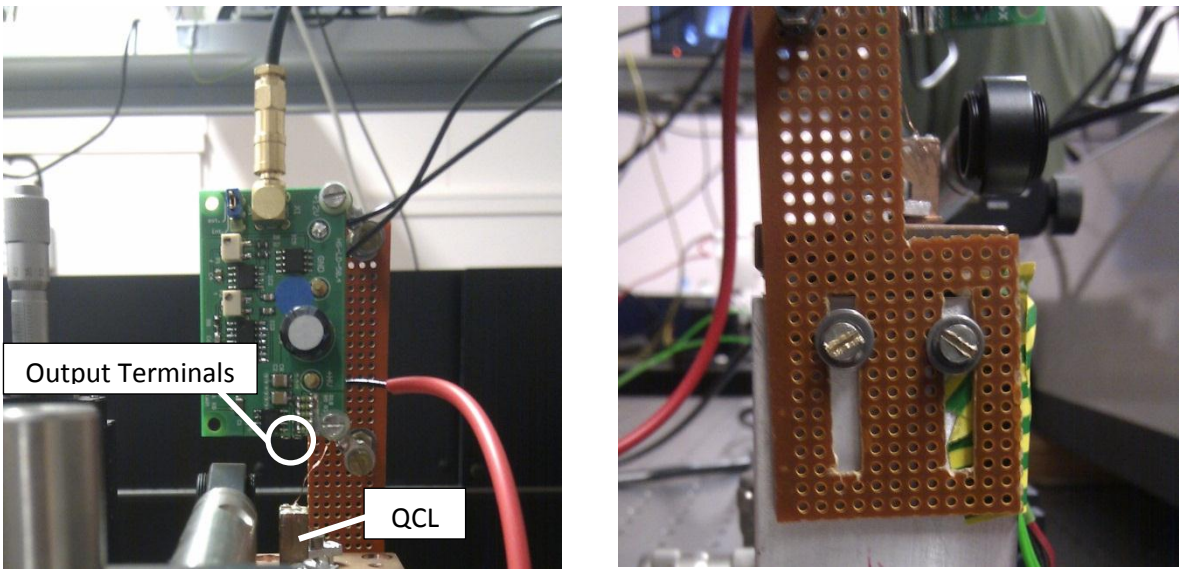

(a) (b)

Figure 23. Showing the mounting system for the Dr Heller OEM pulse driver. (a) shows the unit in a disconnected state mounted above the QCL block. The unit can then be lowered very close (<6mm) to the QCL by adjusting the height screws as depicted in (b).

Initial testing with this device proved very promising, tests across the simulator and with live QCLs showed that the device produced acceptable pulses and was capable of safely powering the QCLs. However not long after being tested using this system one of the samples was rendered inoperable. Further testing showed that the driver was no longer producing the pulses that were first observed; rather a very similar dc source like output was measured as in most of our own custom designed

drivers. After procuring a replacement we found the same issue repeated, these devices were simply to unreliable to continue to use them for an extended time.

After extensive searching and research one other OEM device which was commercially available was identified as potentially offering the features we needed. This device actually produced a very high output even at the short pulse durations we required, so much so that even set at minimum levels it would likely damage or destroy our samples. We were able to overcome this issue by manually altering the device, specifically by de-soldering a number of resistors thereby altering the addressable current range to one which is much better suited to our application field.

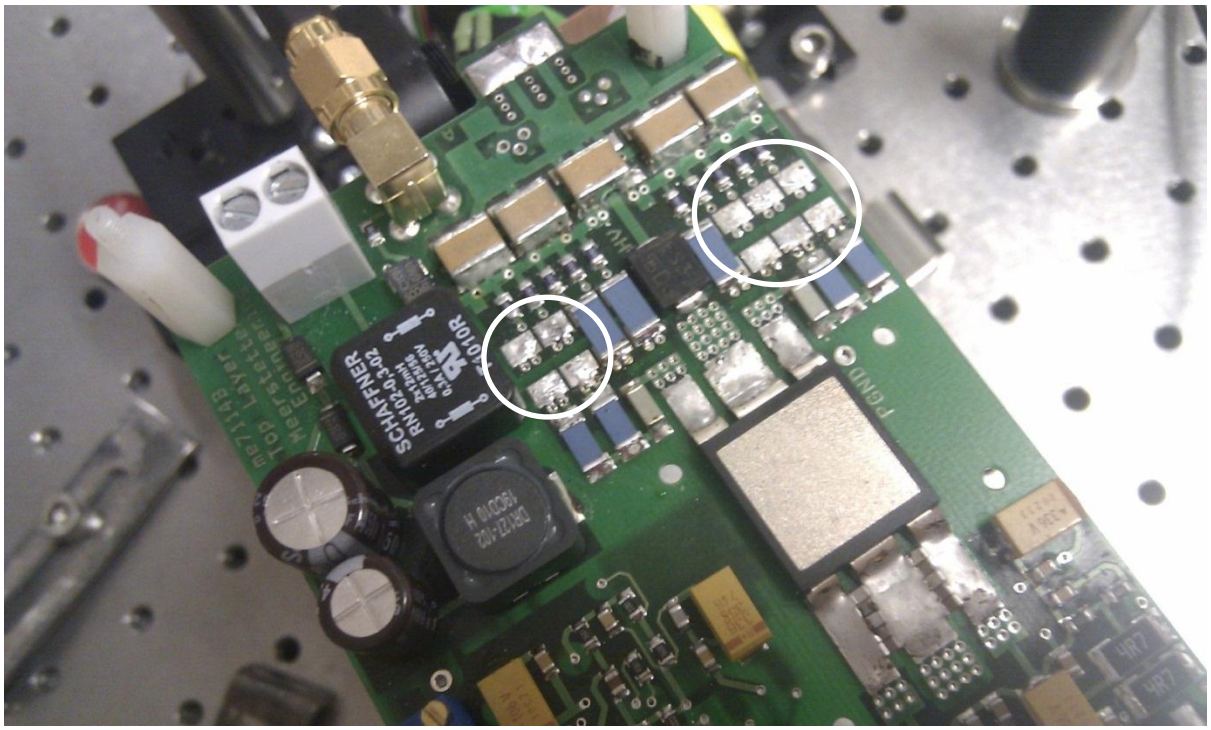

Figure 24. Showing the PCO-7120 with de-soldered resistors.

The new unit also offered a number of other advantages including inbuilt pulse generation up to 5kHz, on-board pulse width control and current generation and most useful of all an integrated current monitor. These features greatly improved the experimental set-up by eliminating the external pulse generator and dc source. It also provided a much easier way of determining current draw across the laser diode improving safety.

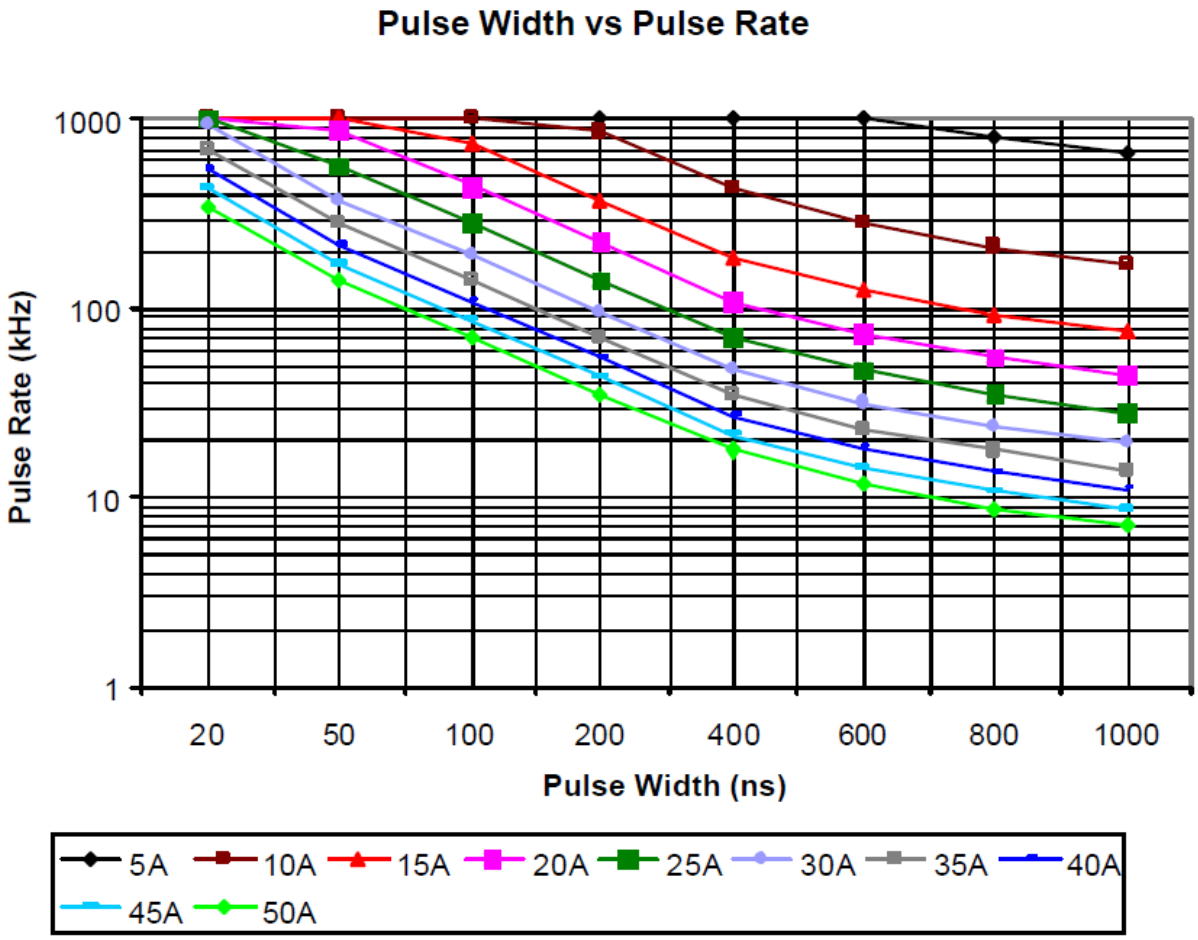

Figure 25. Graph showing maximum output pulse widths and corresponding max frequency from the PCO-7120 (44).

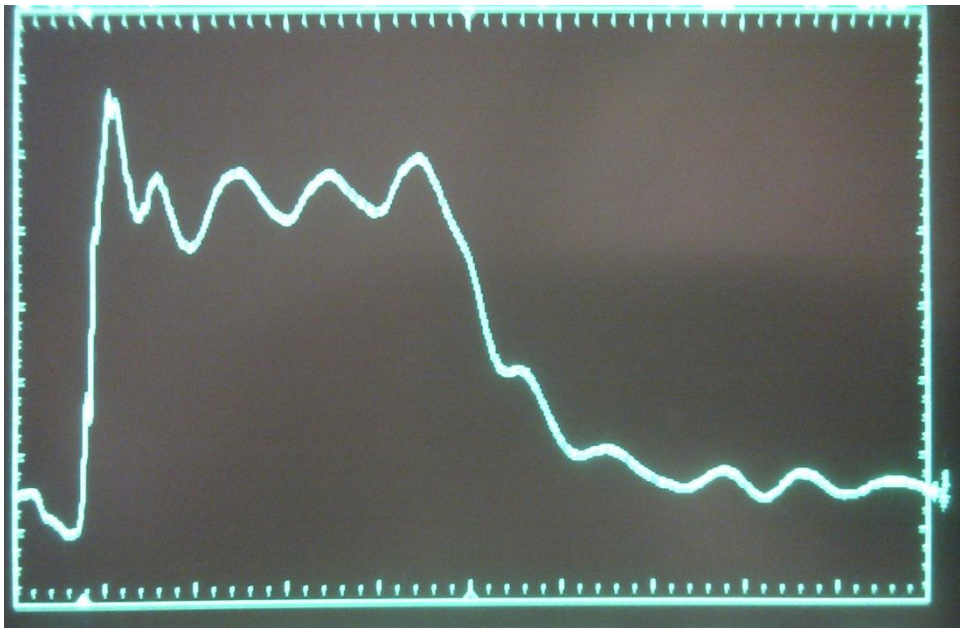

Figure 26. Showing a very good 50ns pulse from Directed Energy Incorporated's PCO-7120.

This modified unit represented the end of our power delivery challenge. We were now able to safely and reliably power our QCLs in any regime we wished.

New Tunable Samples

After the initial successful experimentation with the Fabry-Pérot devices we wanted to work towards a design which would provide much better tunability potential. As previously discussed one of the best designs with regards to tunability incorporates an external-cavity. We therefore had QCLs grown which could accommodate such a set up. Rather than having high reflectivity facets there was an attempt to coat the facets with anti-reflective material which would allow as much light as possible to exit and enter the back facet so that highly selective feedback could take place.

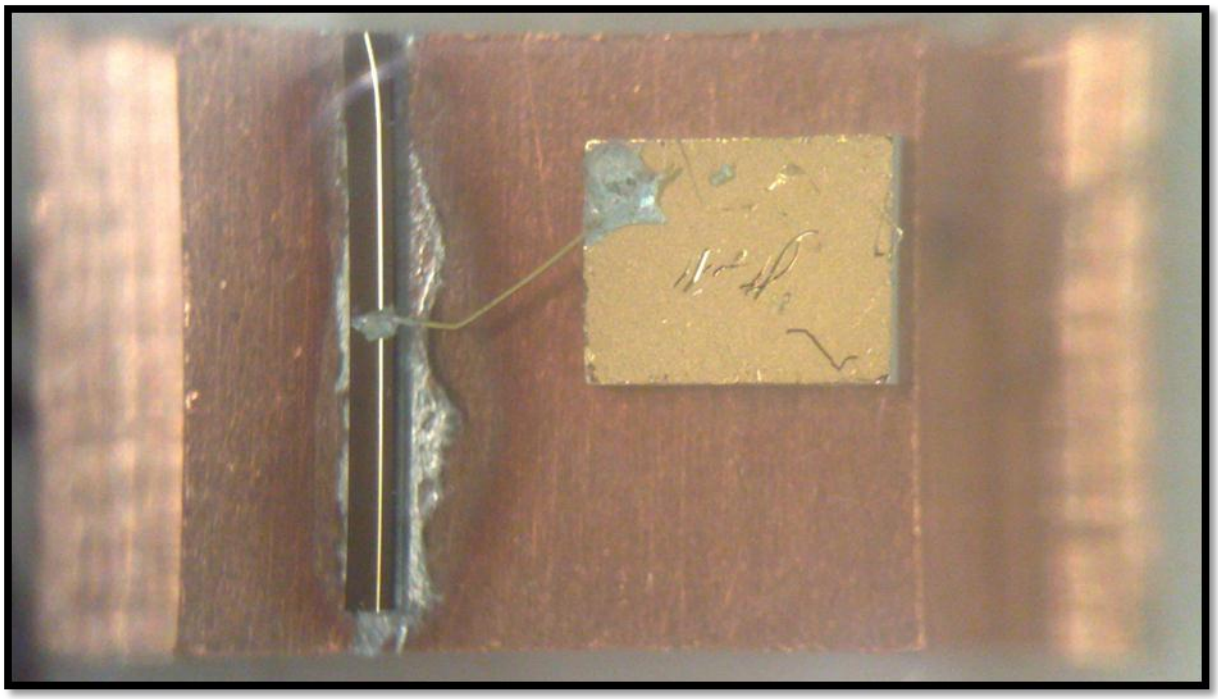

Figure 27. Showing the external-cavity 'tuneable' design of the new QCL. Note the 14° tilt at the rear facet (to the top of the picture).

Another key feature of this new design is that it incorporates a tilt at the rear facet of 7° in some and 14° in others. These tilts are designed to approach the Brewster angle which further minimises reflectance.

The result of these changes is that technically the diode no longer contains a true internal cavity and therefore without feedback at one of the facets a far higher level of current is required to produce detectable output. Where the lasing threshold of the Fabry-Pérot devices was around 600mA some tuneable devices require up to 4A or more.

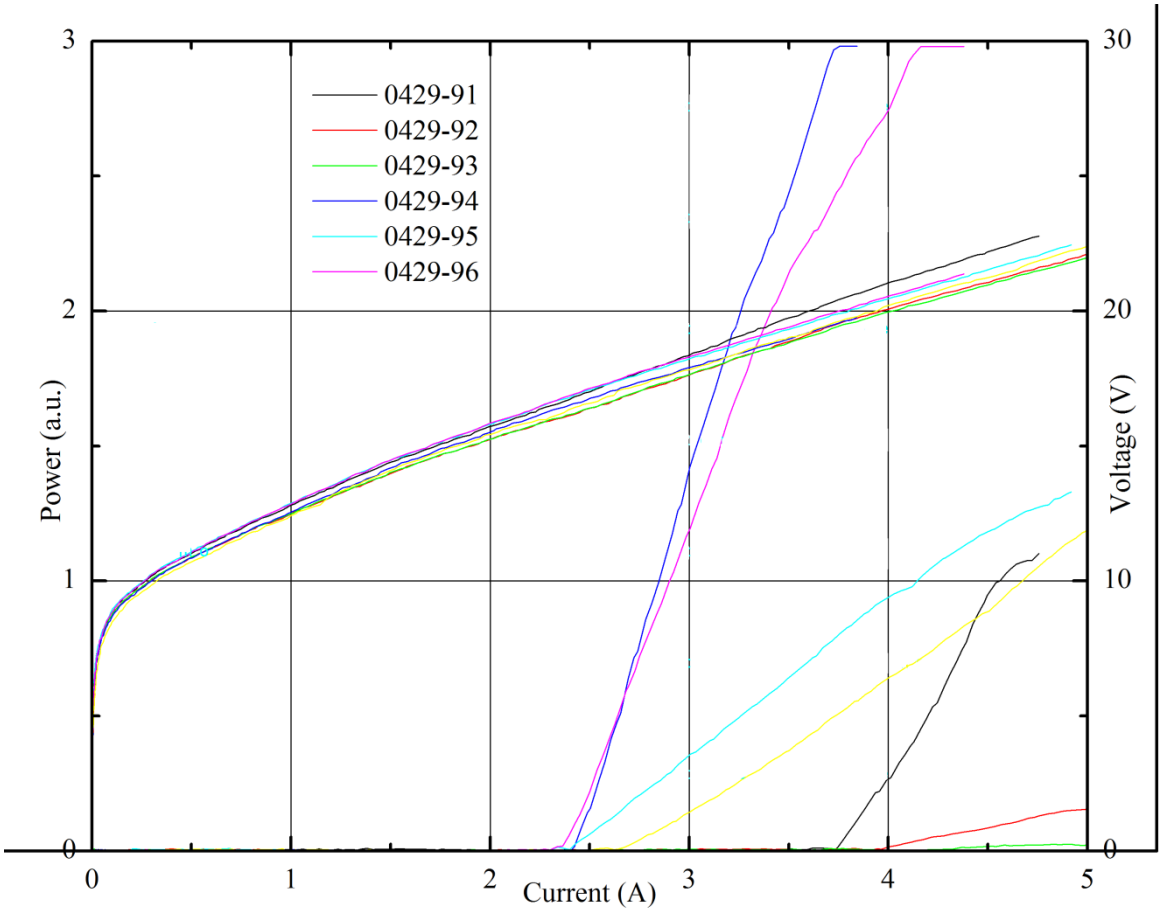

Figure 28. Current, Voltage, Power Graph showing the far higher powers required to operate the external-cavity devices compared to the levels discussed previously in this thesis.

The higher power levels associated with these devices was one of the contributing factors to the driver challenge previously discussed, additional challenges involved designing a system which would allow lenses to be mounted at both facets and allow the driver to be mounted close enough to the diode to deliver rapid pulses.

External-Cavity Experiments

Using this system an attempt was first made to back couple a high reflectivity mirror which reflects light at the working wavelength range to the rear facet. There are a number of external-cavity configurations which have been proposed in literature, the form used in these experiments is the Littrow configuration as this allows the grating (which will eventually take the place of the mirror) to be adjusted and so 'tune' the feedback while sending the output beam back in the same direction.

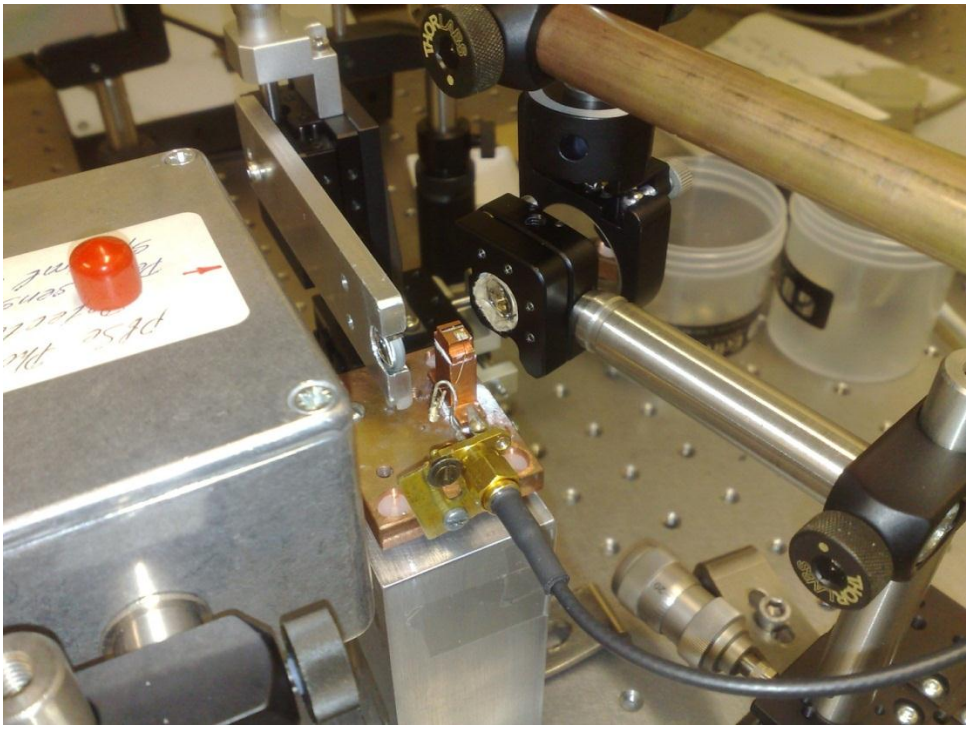

Figure 29. Showing the external-cavity set-up in Littrow configuration with CaF_2 lenses at either facet, a photodiode at the front facet and a high reflectivity mirror at angle on the rear facet.

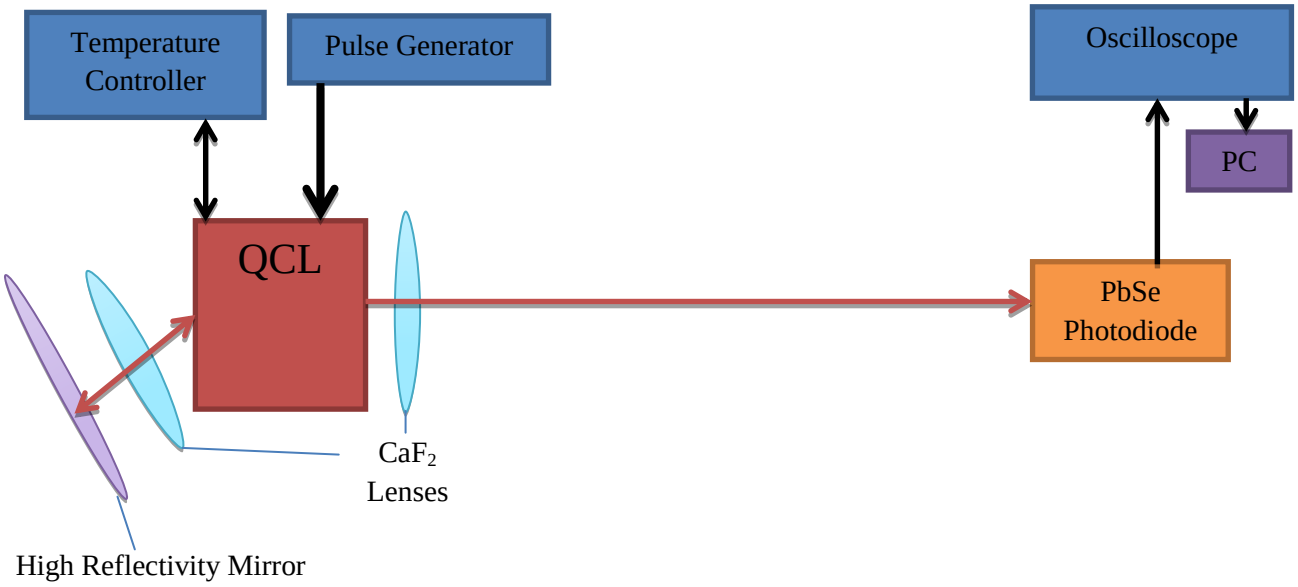

Figure 30. Showing the experimental set-up for the mirror back coupling test. In this case the test sought to observe if feedback was possible with this set-up.

This was deemed an appropriate step as coupling a mirror is significantly easier and quicker compared to coupling a diffraction grating (the eventual aim), while coupling a mirror can afford no tunability it quickly verifies if the system is working correctly, if feedback can be accomplished and should potentially allow the broad lasing spectral output to be easily analysed.

This set-up did prove successful and a proved that the external-cavity set-up would work, however alignment was difficult and imperfect. Before continuing on to the diffraction grating tests it was decided to improve this experimental set-up.

Improving the Set-Up

Emission from all QCLs suffer from a relatively high divergence, additionally before back-coupling the relative optical powers we were dealing with are fairly low. The mirror back-coupling experiment showed these to be very limiting factors. In an effort to overcome both of these challenges it was decided to source some improved lenses.

By using lenses which were aspheric to aid beam collimation and which had a short focal length to allow a maximum amount of light to be captured from the diode facets a great deal more power should be detected at the photodiode site when aligned correctly than with the previously used CaF_2 lenses.

SeGeSb Aspheric lenses were manufactured for us with a 3mm focal length and an infrared anti-reflective coating to improve efficiency.

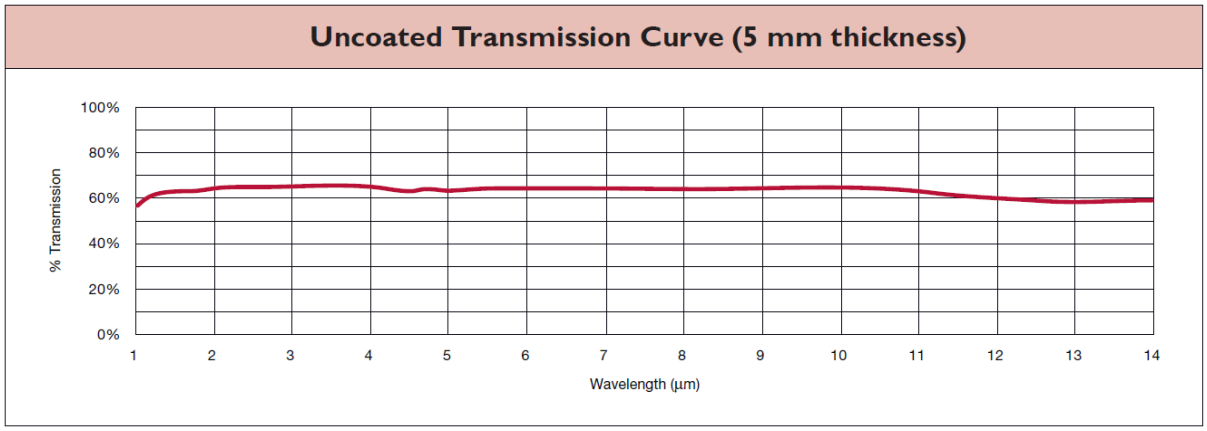

(a)

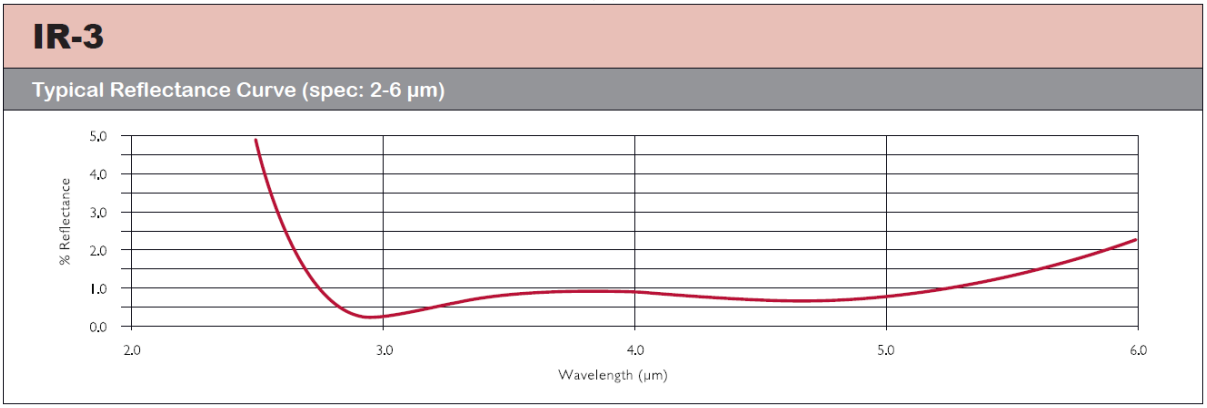

(b)

Figure 31. (a) showing the uncoated transmission curve for the aspheric lenses. (b) showing the reflectance curve for the coating we had applied to the aspheric lenses (44).

The short focal length coupled with the short wire distance between laser and driver required an improved physical set up to accommodate these entities around the diode and still allow lens movement for alignment and access to the diode for connection and disconnection. Initially the driver was mounted horizontally and closely to the diode with the aspheric lenses in standard mounts mounted on xyz stages and on arms which were inserted into place either side of the diode. It was found that in this set up there was not enough room to effectively align the lenses and the driver was slightly too far away from the diode to produce the very nice pulses we would like. The set-up was therefore altered to allow the driver to be mounted vertically much like the original Dr. Heller set up. This new design allows good access to the diode, very close driver connection and perfect freedom around either facet for lens alignment.

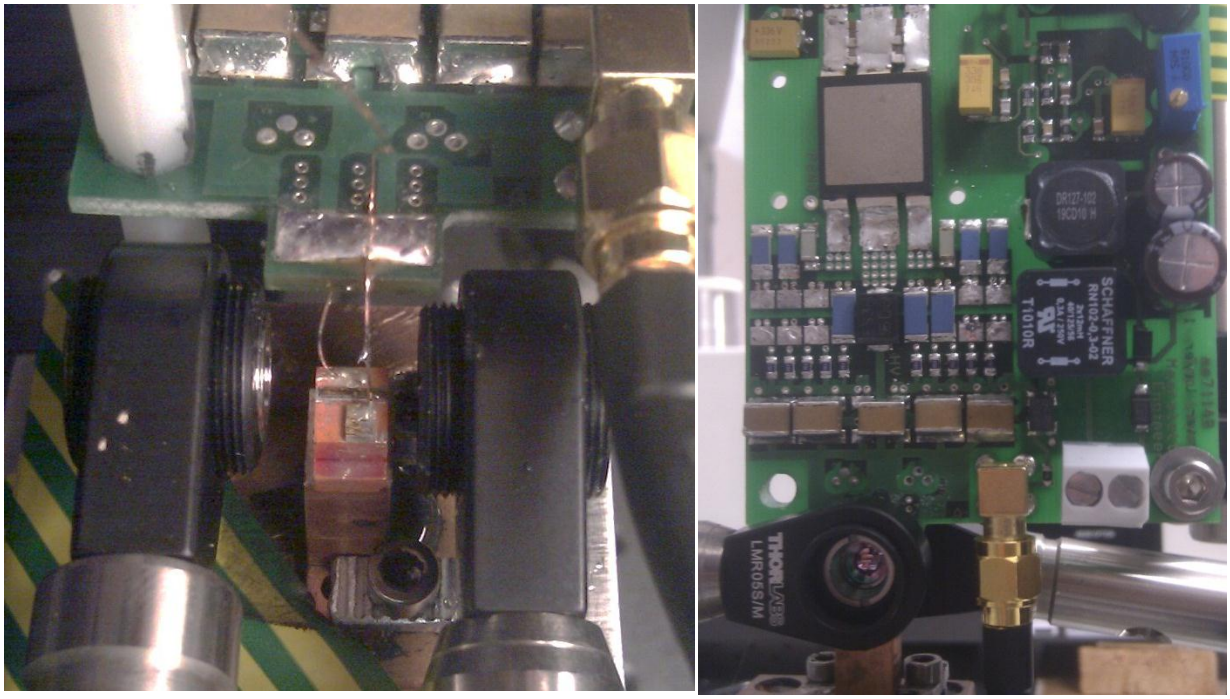

(a) (b)

Figure 32. Showing the original set-up (a) which did not provide enough freedom and poor pulse shapes. (b) shows one side of the vertical set-up which allows complete freedom and exceptional pulse shapes.

This new set up made alignment much easier and detected powers were much higher. Because back-coupling would be so pivotal to the next external-cavity stage alignment of the rear beam was critical.

Aligning a ~3.3µm beam is very challenging mainly because there is no way to visualise a beam of this wavelength, although thermal imaging solutions exist they are ineffective with so little average power. The only way to effectively align the beam was to use the PbSe photodiode already discussed. However due to the size and bulk of the photodiode housing it was impossible to position the diode into positions where it would be useful. A slight change to the photodiode circuit and by mounting the diode within a lens holder and post system we were able to produce a vastly more effective alignment tool.

Figure 33. Improved PbSe Photodiode system, here the diode is mounted in a lens holder and can be positioned in the exact position where the laser beam should enter the monochromator. Alignment can then take place to maximise photodiode response before removing the photodiode and allowing the aligned laser light to enter the monochromator.

Repeating the previous mirror test with the improved system and tools yielded vastly more impressive results. When aligned a large amount of incident energy on the photodiode was recorded, this photodiode sat at the front facet. When the rear facet was occluded the incident energy detected on the photodiode dropped by orders of magnitude - though some energy was still detected during pulse phases of course. These results showed that feedback and lasing was definitely taking place in the external-cavity set-up.

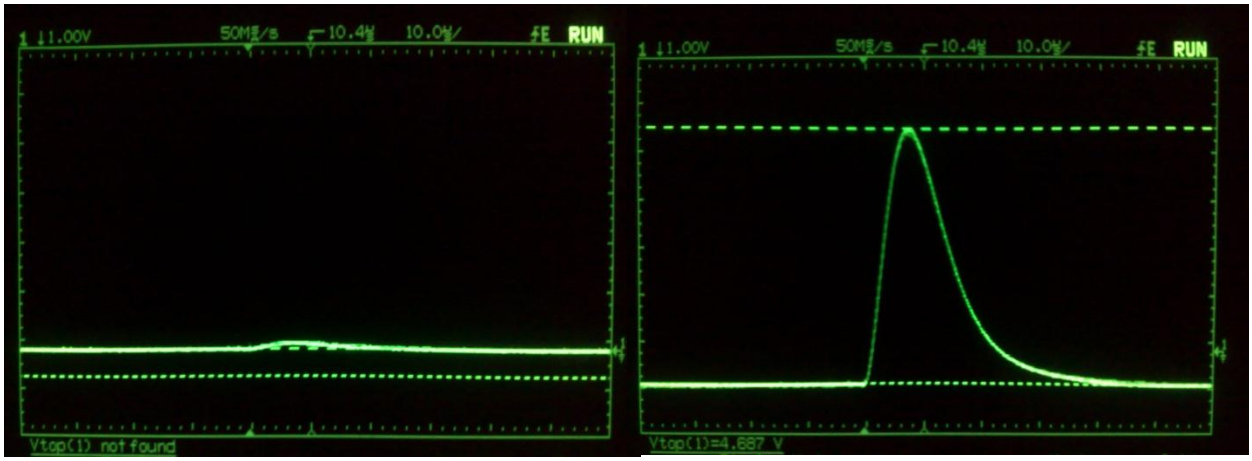

(a) (b)

Figure 34. (a) showing the photodiode output when the rear facet is occluded. (b) shows the exact same conditions only a moment later when the rear facet is uncovered.

This set-up was then used to examine the emitted spectrum of the device in this state. A half meter monochromator was placed between the QCL and photodiode and controlled via PC as previously discussed.

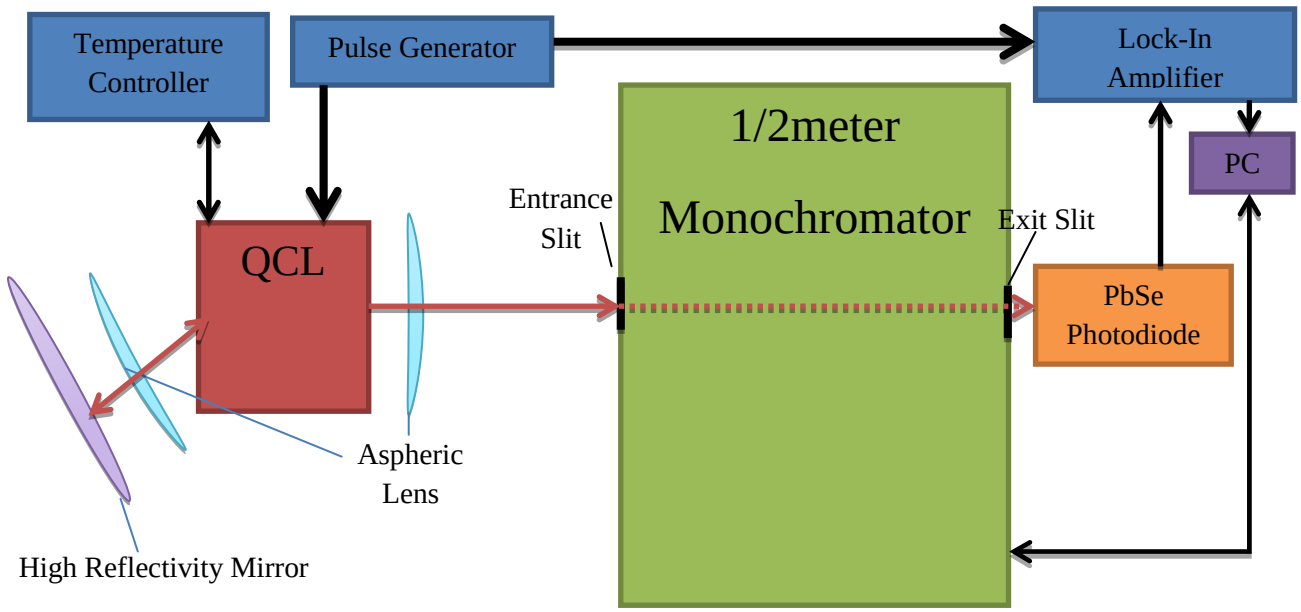

Figure 35. Showing experimental set-up diagram for the back-coupled mirror broad lasing spectral output study.

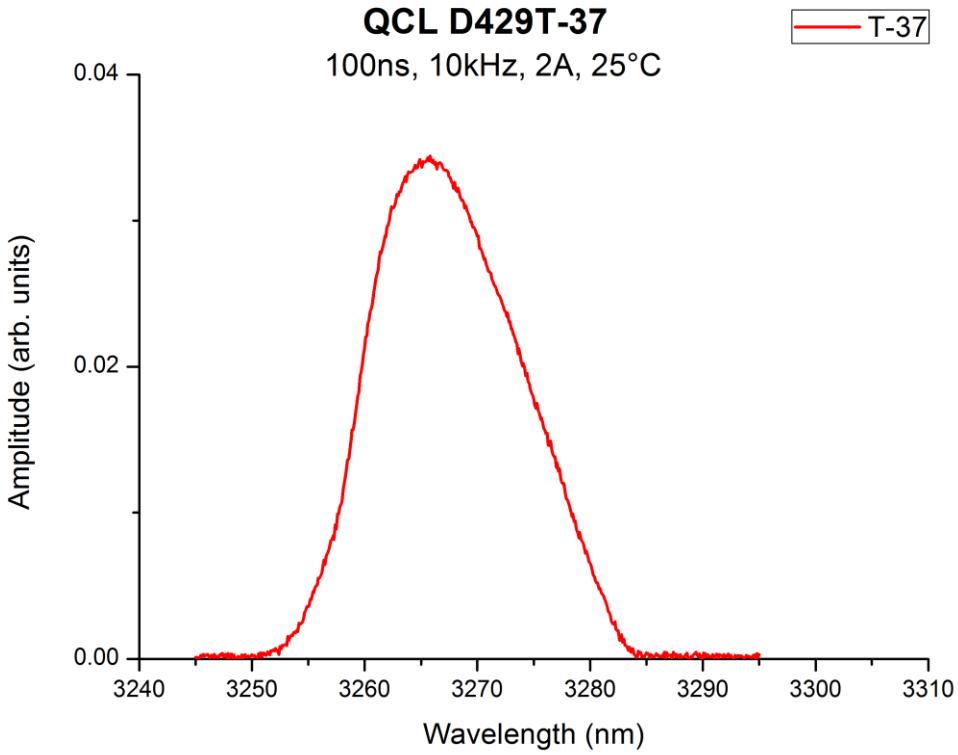

Figure 36. Showing the broad lasing spectral output from one of the QCLs in external-cavity arrangement with a high reflectivity mirror back-coupled to the rear facet.

These experiments verified that the external-cavity system worked and that the central wavelengths of the QCLs we were working with were at the desirable region we were looking for.

Diffraction Grating Selection

Appropriate selection and design of the diffraction grating is vital if an efficient external-cavity system is to be built.

A diffraction grating is essentially a plane with a periodic structure that diffracts light by varying degrees depending on wavelength. There are a variety of gratings and manufacturing techniques, we had a common reflective ruled diffraction manufactured for us. The grating had 300 grooves/mm and a 4µm blaze which provided the following efficiencies.

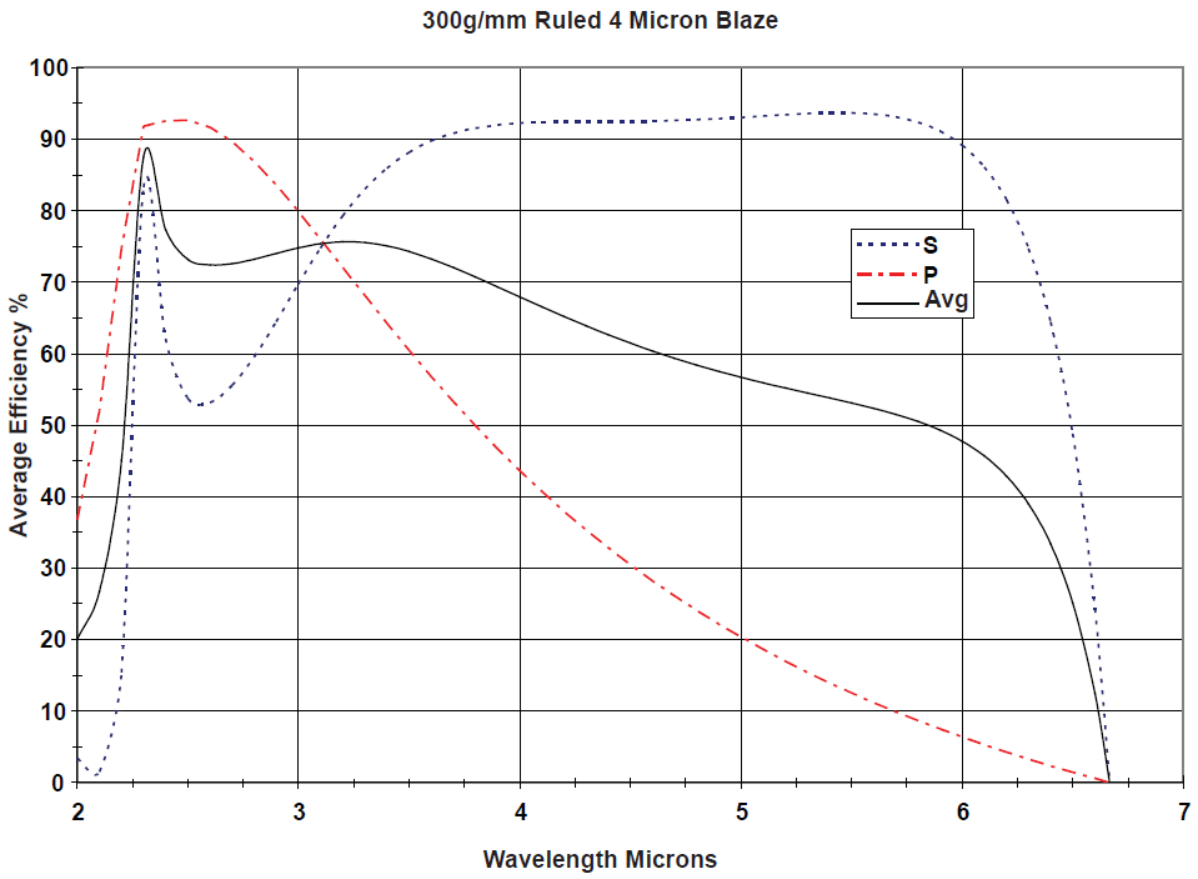

Figure 37. Graph showing the efficiency of the grating selected for the external-cavity set-up. Adapted from (45).

At the wavelength range we are investigating this grating gives good efficiency both in perpendicular and parallel polarisation.

While the theory of operation of diffraction gratings is extremely well understood and fully predictable using mathematical equations in practical application to the experimental set-up this precise information is of little value as the precise angle of the QCL beam is not known. It was far quicker to use initial approximations and subsequently use trial-and-error methods of alignment to back-couple the diffraction grating to the rear facet.

At the time of writing all that remains is to run a series of monochromator passes such as those already conducted and described and discussed with the diffraction grating at different angles to selectively feedback precise wavelengths. The results will reveal the tuning range of these novel devices.

Conclusions

The main focus of these studies was to determine if novel QCL technology could take the place of OPO sources in a real-time video-rate gas imaging system. For this to be true the QCL would need to exhibit a number of features. A repetition rate of at least 5kHz was desirable; rep rates exceeding even the most demanding applications were successfully observed. Pulse widths of at least 5ns would be necessary; pulse widths of 50ns are effortlessly produced by these samples and these can be lengthened if necessary. The QCL must be able to operate without the need for liquid cooling or any other bulky/expensive system; all of our experiments were conducted for extended periods of time at room temperature – if necessary Peltier based devices can be used for thermal control, these are fairly small and inexpensive.

A highly desirable outcome would be if it were shown that these QCL devices were also able to be tuned to a degree. The literature has proven that external-cavity set-ups with QCLs produce good tunability; we have shown that our revised samples with anti-reflective coated facets and tilted rear facets can be used in an external-cavity set-up and that therefore tunability is possible by manipulation of a diffraction grating in a Littrow configuration external-cavity set-up.

In short we have shown that QCLs are an ideal replacement for the expensive, delicate and bulky OPO sources.

Thermal Issues

Throughout the experiments a number of devices were observed to degrade and sometimes rendered inoperable despite being well maintained and not being stressed electrically or physically. It is speculated that as suggested by much literature and previous quantum cascade laser research that the main reason for this is likely to be thermal damage caused by highly localised heat build-up during high current/long pulse/high frequency operation, Chaparala et al. note several thermal performance issues that are likely to have been encountered by these quantum cascade lasers (47).

Subsequently the same group developed thermal models for QCLs which were very similar to those experimented on showing that the proposed thermal issues are likely to have produced a degradation in lasing output that ultimately leads to laser failure, a number of thermal management suggestions are made in terms of design and manufacture (48).

It should be noted that these issues occur in regimes which are far more demanding on the QCLs than any standard real-time video-rate gas imaging system would require.

Future Work

We are already on the verge of determining precisely the tuning range of these devices; we need only complete a series of tests using a back-coupled diffraction grating as previously discussed. An improved version of these tests might incorporate computer control to assess and operate precisely the angle of the tuning grating and thus record and run many test series autonomously.

Thermal management improvements can be made experimentally by using a smaller Peltier platform which would track temperature changes more accurately. In a similar vein the thermocouple responsible for thermal monitoring could be mounted much closer to the active area of the laser diode. Additionally in some set-ups there were many thermal junctions between the thermocouple, Peltier platform and laser diode due to the diode being mounted on secondary or tertiary mounts in order to achieve a height where access to the diode was possible. A fully customised platform would allow the laser diode to be mounted directly onto the Peltier platform.

From a design/manufacture standpoint there are a number of improvements which have been suggested by Chaparala et al. though not all of these are possible or applicable; some of the most recent QCLs grown for us in Sheffield utilise a different mounting method that allows the active area to be in closer contact with cooling materials.

Bibliography

1. **Steen, W. M.** *Laser Materials Processing.* 1998. Vol. 2nd Ed.

2. *The LASER, Light Amplification by Stimulated Emission of Radiation.* **Gould, R. Gordon.** University of Michigan : Franken, P.A. and Sands, R.H. (Eds.), 1959. The Ann Arbor Conference on Optical Pumping.

3. **al, WR Bennett et.** *Gas Optical Maser. US Patent 3,149,290* United States of America, 15 September 1964.

4. **Palmer, Jason.** Laser is produced by a living cell. *BBC News.* [Online] 13 06 2011. [Cited: 13 06 2011.] http://www.bbc.co.uk/news/science-environment-13725719.

5. *Single-cell biological lasers.* **Gather, Malte C.** s.l. : Nature Photonics, 2011. doi:10.1038/nphoton.2011.99.

6. *Possibility of amplification of electromagnetic waves in a semiconductor with a superlattice.* **Kazarinov, R.F and Suris, R.A.** 4, s.l. : Fizika i Tekhnika Poluprovodnikov, April 1971, Vol. 5, pp. 797–800.

7. *Quantum Cascade Laser.* **Faist, Jerome and Federico Capasso, Deborah L. Sivco, Carlo Sirtori, Albert L. Hutchinson, and Alfred Y. Cho.** (5158), s.l. : Science, April 1994, Vol. 264, pp. 553–556. Bibcode 1994Sci...264..553F.

8. *High-performance midinfrared quantum cascade lasers.* **Capasso, Federico.** 11, s.l. : Optical Engineering, 2010, Vol. 49.

9. **Dr. Quankui Yang, Christian Manz, Dr. Wolfgang Bronner, Dr. Klaus Köhler and Joachim Wagner.** Short-Wavelength Quantum-Cascade Lasers. *Photonics.com.* [Online] 01 04 2007. [Cited: 2010 06 05.] http://www.photonics.com/Content/ReadArticle.aspx?ArticleID=29075.

10. *Time-resolved spectral characteristics of external-cavity quantum cascade lasers and their application to stand-off detection of explosives.* **B. Hinkov, F. Fuchs, Q.K. Yang, J.M. Kaster, W. Bronner, R. Aidam, K. Köhler, J.Wagner.** 253-260, s.l. : Applied Physics B: Lasers and Optics, 2010, Vol. 100. DOI 10.1007/s00340-009-3863-7.

11. *High power quantum cascade lasers.* **Manijeh Razeghi, Steven Slivken, Yanbo Bai, Burc Gokden and Shaban Ramezani Darvish.** 12, s.l. : New Journal of Physics, 2009, Vol. 11. doi:10.1088/1367-2630/11/12/125017.

12. *High-average-power, high-duty-cycle (λ ~ 6 µm) quantum cascade lasers.* **Slivken, S. and A. Evans, J. David, and M. Razeghi.** 23, s.l. : Applied Physics, 2002, Vol. 81. doi:10.1063/1.1526462.

13. **Jones-Bey, Hassaun A.** Quantum-cascade lasers smell success. *Laser Focus World.* [Online] 01 03 2005. [Cited: 03 06 2011.] http://www.optoiq.com/index/display/article-

display/224013/articles/laser-focus-world/volume-41/issue-3/optoelectronics-world/quantum-cascade-lasers-smell-success.html.

14. *Broadband tuning of external cavity bound-to-continuum quantum-cascade lasers.* **Maulini, Richard and Mattias Beck, Jérome Faist, and Emilio Gini.** 10, s.l. : Applied Physics Letters, 2004, Vol. 84. doi:10.1063/1.1667609.

15. **World, Laser Focus.** Alpes offers CW and pulsed quantum cascade lasers. *Laser Focus World.* [Online] 19 04 2004. [Cited: 23 06 2011.]

16. **WEIDA, MILES J.** Tunable QC laser opens up mid-IR sensing applications". *Laser Focus World.* [Online] 01 07 2006. [Cited: 23 06 2011.] http://www.optoiq.com/index/display/article-display/259939/articles/laser-focus-world/volume-42/issue-7/optoelectronics-world/tunable-qc-laser-opens-up-mid-ir-sensing-applications.html.

17. *Room temperature quantum cascade lasers with 27% wall plug efficiency.* **Bai, Y., Bandyopadhyay, N., Tsao, S., Slivken, S., Razeghi, M.** 18, s.l. : Applied Physics Letters, 2011, Vol. 98. DOI: 10.1063/1.3586773.

18. *Multi-watt level short wavelength quantum cascade lasers.* **Lyakh, A., Maulini, R., Tsekoun, A.G., Go, R., Patel, C.K.N.** 79531L , s.l. : Proceedings of SPIE - The International Society for Optical Engineering, 2011, Vol. 7953. DOI: 10.1117/12.872739.

19. *Room-temperature continuous wave operation of distributed feedback quantum cascade lasers with watt-level power output.* **Lu, Q.Y., Bai, Y., Bandyopadhyay, N., Slivken, S., Razeghi, M.** 23, s.l. : Applied Physics Letters, 2010, Vol. 97. DOI: 10.1063/1.3525859.

20. *Wavelength tuning of GaAs/AlGaAs terahertz quantum cascade lasers by controlling aluminum content in barriers.* **Samal, N.a , Sadofyev, Y.G.a , Annamalai, S.a , Chen, L.a , Samal, A.a , Johnson, S.R.b.** 1, s.l. : Journal of Crystal Growth, 2011, Vol. 323. DOI: 10.1016/j.jcrysgro.2010.10.134.

21. *Room Temperature CW Operation of Short Wavelength Quantum Cascade Lasers Made of Strain Balanced GaInAs/AlInAs Material on InP Substrates.* **Xie, F., Caneau, C., LeBlanc, H.P., Visovsky, N.J., Chaparala, S.C., Deichmann, O.D., Hughes, L.C., Zah, C.-e., Caffey, D.P., Day, T.** s.l. : IEEE Journal on Selected Topics in Quantum Electronics, 2011. DOI: 10.1109/JSTQE.2011.2136325.

22. *Single-mode tunable, pulsed, and continuous wave quantum-cascade distributed feedback lasers at $\lambda \cong 4.6\text{-}4.7\ \mu m$.* **Köhler, R.a b , Gmachl, C.b , Tredicucci, A.b , Capasso, F.b , Sivco, D.L.b , Chu, S.N.G.b , Cho, A.Y.** 9, s.l. : Applied Physics Letters, 2000, Vol. 76. ISSN: 00036951.

23. *Si/SiGe heterostructures: from material and physics to devices and circuits.* **Paul, Douglas J.** 75, s.l. : Semicond. Sci. Technol, 2004, Vol. 16. doi: 10.1088/0268-1242/19/10/R02.

24. *State of art of IV-VI semiconductor light emitting devices in mid infrared opto-electronic applications.* **S. Mukherjee, and Z. S. Shi.** 236-245, s.l. : IETE Technology Review, 2009, Vol. 26.

25. *High-Performance InP-Based Mid-IR Quantum Cascade Lasers.* **Razeghi, Manijeh.** 3, s.l. : IEEE JOURNAL OF SELECTED TOPICS IN QUANTUM ELECTRONICS, 2009, Vol. 15.

26. *3 W continuous-wave room temperature single-facet emission from quantum cascade lasers based on nonresonant extraction design approach.* **A. Lyakh, R. Maulini, A. Tsekoun, R. Go, C. Pflügl, L. Diehl, Q. J. Wang, Federico Capasso, and C. Kumar N. Patel.** s.l. : Applied Physics Letters, 2009, Vol. 95. doi:10.1063/1.3238263.

27. *High-temperature operation of distributed feedback quantum-cascade lasers at 5.3 μm.* **D. Hofstetter, M. Beck, T. Aellen, and J. Faist.** 396, s.l. : Applied Physics Letters, 2001, Vol. 78. doi:10.1063/1.1340865.

28. *DFB Quantum Cascade Laser Arrays.* **Lee, B.G. Belkin, M.A. Pflugl, C. Diehl, L Zhang, H.A Audet, R.M. MacArthur, J. Bour, D.P. Corzine, S.W. Hufler, G.E. Capasso, F.** 5, s.l. : IEEE Journal of Quantum Electronics, 2009, Vol. 45. 10.1109/JQE.2009.2013175.

29. *Recent progress in quantum cascade lasers and applications.* **Claire Gmachl, Federico Capasso, Deborah L Sivco and Alfred Y Cho.** 11, s.l. : Reports on Progress in Physics, 2001, Vol. 64. doi: 10.1088/0034-4885/64/11/204.

30. *External cavity quantum cascade laser tunable from 7.6 to 11.4micrometer.* **Andreas Hugi, Romain Terazzi, Yargo Bonetti, Andreas Wittmann, Milan Fischer, Mattias Beck, Jérôme Faist and Emilio Gini.** s.l. : APPLIED PHYSICS LETTERS, 2009, Vol. 95. DOI: 10.1063/1.3193539.

31. *Heterogeneous High-Performance Quantum-Cascade Laser Sources for Broad-Band Tuning.* **Wittmann, A, Hugi, A, Gini, E, Hoyler, N. Faist, J.** 11, s.l. : IEEE Journal of Quantum Electronics, 2008, Vol. 44. 10.1109/JQE.2008.2001928 .

32. **M-Squared Lasers.** Firefly-IR. *M-Squared Lasers.* [Online] 01 01 2011. [Cited: 04 07 11.] http://www.m2lasers.com/products-services/laser-systems/firefly-ir.aspx.

33. *Hyperspectral imaging of gases with a continuous-wave pump-enhanced optical parametric oscillator.* **David J. M. Stothard, Malcolm H. Dunn, Cameron F. Rae.** 5, s.l. : Optics Express, 2004, Vol. 12. DOI: 10.1364/OPEX.12.000947.

34. **M. Ebrahimzadeh and M. H. Dunn.** Optical Parametric Oscillators. *OSA Handbook of Optics.* 2001.

35. *Continuous-wave singly resonant pump-enhanced type II.* **G. Robertson, M. J. Padgett, and M. H. Dunn.** 1735-37, s.l. : Optics Letters, 1994, Vol. 19.

36. *Single-frequency mid-infrared optical parametric oscillator source.* **F. Hanson, P. Poirier and M. A. Arbore.** 1794-96, s.l. : Optics Letters, 2001, Vol. 26.

37. *High resolution Doppler-free molecular spectroscopy with a continuous-wave optical parametric oscillator.* **E. V. Kovalchuk, D. Dekorsy, A. I. Lvovsky, C. Braxmaier, J. Mlynek, A. Peters and S. Schiller.** 1430-32, s.l. : Optics Letters, 2001, Vol. 26.

38. *Transportable, highly-sensitive photoacoustic spectrometer based on a continuous-wave dual-cavity optical parametric oscillator.* **F. Muller, A. Popp, F. Kuhnemann and S. Schiller.** 2820-25, s.l. : Optics Express, 2003, Vol. 11.

39. *Photoacoustic trace gas detection using a cw single-frequency optical parametric oscillator.* **F. Kuhnemann, K. Schneider, A. Hecker, A. A. E. Martis, W. Urban, S. Schiller and J. Mlynek.** 741-45, s.l. : Applied Physics, 1998, Vol. 75.

40. *High temperature operation of 3.3micrometer quantum cascade lasers.* **J. Devenson, O. Cathabard, R. Teissier, and A. N. Baranov.** 141106, s.l. : APPLIED PHYSICS LETTERS, 2007, Vol. 91. DOI: 10.1063/1.2794414.

41. *InGaAs/AlAsSb/InP strain compensated quantum cascade lasers.* **Revin, D. G. Cockburn, J. W. Steer, M. J. Airey, R. J. Hopkinson, M. Krysa, A. B. Wilson, L. R. Menzel, S.** 15, s.l. : Applied Physics Letters, 2009, Vol. 90. 10.1063/1.2721125.

42. *Very short wavelength (λ = 3.1–3.3 μm) quantum cascade lasers.* **J. Devenson, D. Barate, O. Cathabard, R. Teissier, and A. N. Baranov.** 19, s.l. : Applied Physics Letters, 2006, Vol. 89. doi:10.1063/1.2387473.

43. **Hamamatsu.** Solid-state Division: Two-color Detector. *Hamamatsu Sales.* [Online] 2011. [Cited: 15 07 2011.] http://sales.hamamatsu.com/assets/pdf/parts_K/k1713-01_etc_kird1029e06.pdf.

44. **Directed Energy Incorporated.** Directed Energy Inc. PCO-7120 User Manual. *Directed Energy Inc.* [Online] 2011. http://www.directedenergy.com/pdf/pco-7120_manual.pdf.

45. **LightPath Ltd.** LightPath Catalog. *LightPath.* [Online] [Cited: 16 07 2011.] http://www.lightpath.com/literature/catalog/LightPath_Catalog_Infrared_Optics_Overview.pdf.

46. **Optometrics.** Reflective Diffraction Gratings. *Optometrics.* [Online] [Cited: 07 07 2011.] http://www.optometrics.com//App_Themes/optometrics/pdfs/gratings/300g-mm%204%20micron.PDF.

47. *Thermal management of mid-infrared (IR) quantum cascade lasers.* **Chaparala, S.C., Feng Xie, Caneau, C., Hughes, L.C., Chung-en Zah.** 693-699, s.l. : Electronic Components and Technology Conference (ECTC), 2010 Proceedings 60th, 2010, Vol. 60. 10.1109/ECTC.2010.5490787 .

48. *Design Guidelines for Efficient Thermal Management of Mid-Infrared Quantum Cascade Lasers.* **Chaparala, S. C. Xie, F. Caneau, C. Zah, C. E. Hughes, L. C.** 99, s.l. : IEEE Transactions on Components, Packaging and Manufacturing Technology, 2011, Vol. PP. 10.1109/TCPMT.2011.2142309.

Appendix A

Software Design

A number of software programmes were developed during the project mainly for data recording, command and control of equipment and autonomous testing. This appendix will briefly describe the operation of two of these programmes, the autonomous testing system and the monochromator command and control programme. Examples of the code written for these programmes are given in Appendix B.

Automated Testing

A program was developed which would allow the external Agilent pulse generator to be controlled in software. This gave the immediate advantage of allowing any recorded results to also have the driving conditions recorded accurately. The system also allowed batch tests to be run so for instance a series of tests where the driving conditions were kept constant but the frequency was slowly ramped up from 5kHz to 100kHz could be conducted and the results recorded to show the effect of frequency on peak optical power. Depending on the frequency steps such a series of tests may take many man hours to complete but the automated system could be relied upon to complete these tests and accurately record results without intervention. The system allowed any variable condition or number of variables to be altered in batch runs.

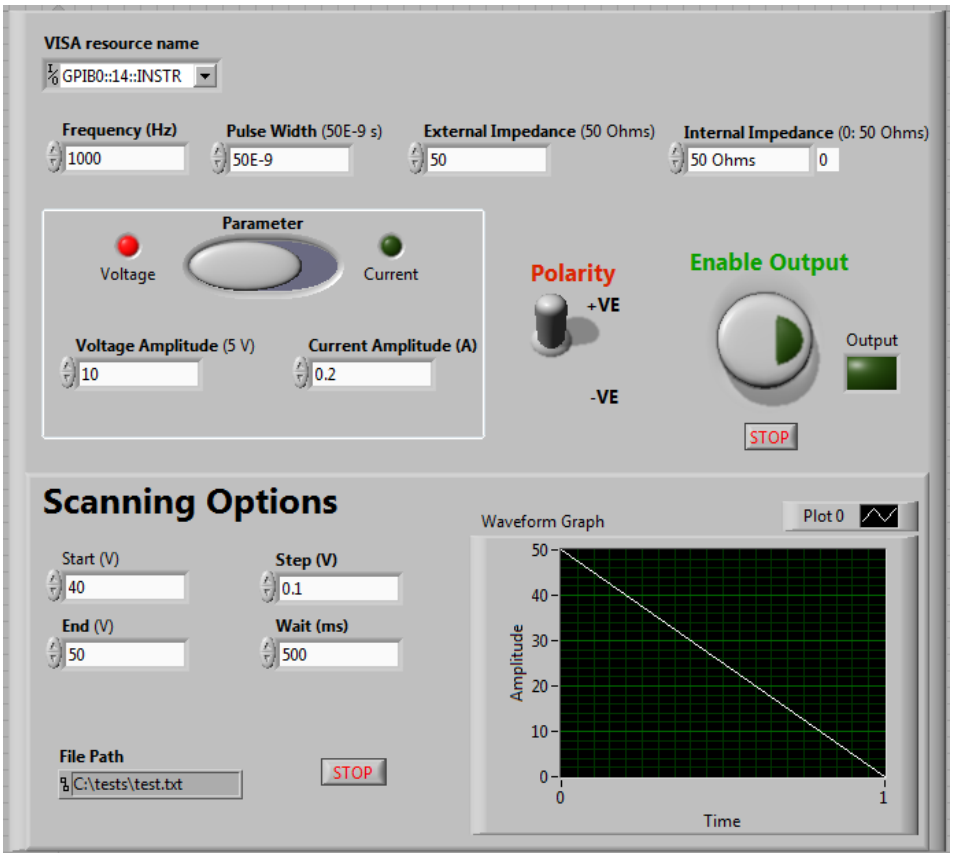

Figure 38. Showing one of the front interfaces for the automated testing system. In this mode all features can be accessed in software including a simple 'batch' scan interface and a waveform representation of output pulses (unavailable on the physical device). More advanced batch runs were loaded in via a configuration file.

Monochromator Control

The spectral scans which we wished to perform required that many iterations of a light pass through the monochromator needed to be conducted. Rather than performing each one manually, recording the results and compiling the data at the end (a very laborious and tedious activity) a software program was developed which automatically and very rapidly allowed the many light passes to be conducted without intervention.

One advantage of designing this software was the opportunity to render grating angles as their wavelength counterpart in the program labels and output. For instance the user could stipulate which wavelength the grating should allow to 'pass' through the monochromator rather than which angle the grating should be set to. This saved a great deal of time as the user did not have to do any diffraction calculations; similarly output was rendered in the wavelength form rather than in grating

angle. The software was designed in two parts, the first allowed initial settings to be dictated such as the primary grating to be used, the exit and entry slit width etc.

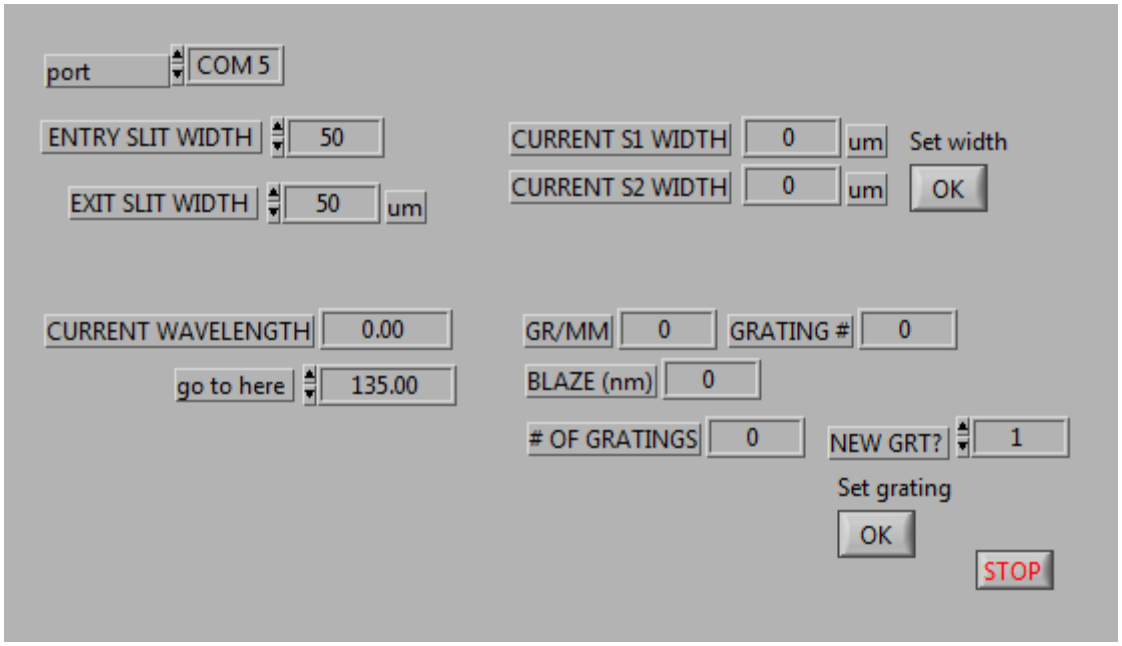

Figure 39. Showing the control section of the monochromator control system. From here slit widths can be monitored and altered, the current wavelength to be passed can be set and the primary grating can be selected and its features noted.

The second part allowed the spectral scan settings to be adjusted. A start and end wavelength could be set as well as the size of the step to be taken between these points. In this way very rapid 'low resolution' scans could be conducted or longer high resolution scans could be conducted when necessary. A highly convenient waveform window would show an instant analysis and spectral graph when the scan was complete. Datafiles were saved and could be subject to further analyses later.

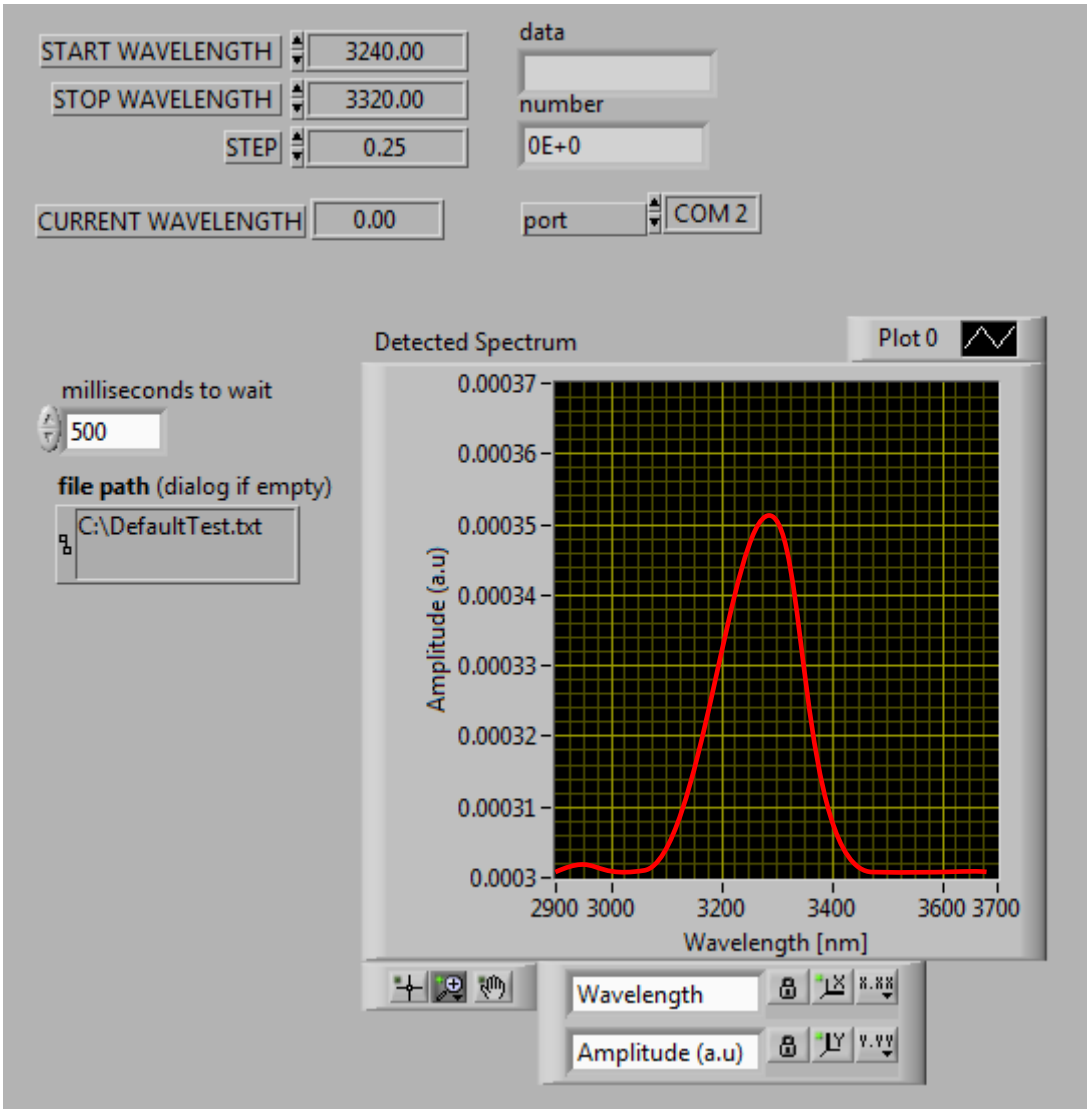

Figure 40. Showing the spectral scan section of the monochromator scan program. Here the spectrum to be scanned can be set including the size of the steps to increase/decrease resolution/speed. An instant preview pane gives immediate analysis of the results without any human intervention.

Appendix B

Code Examples for Automated Testing System

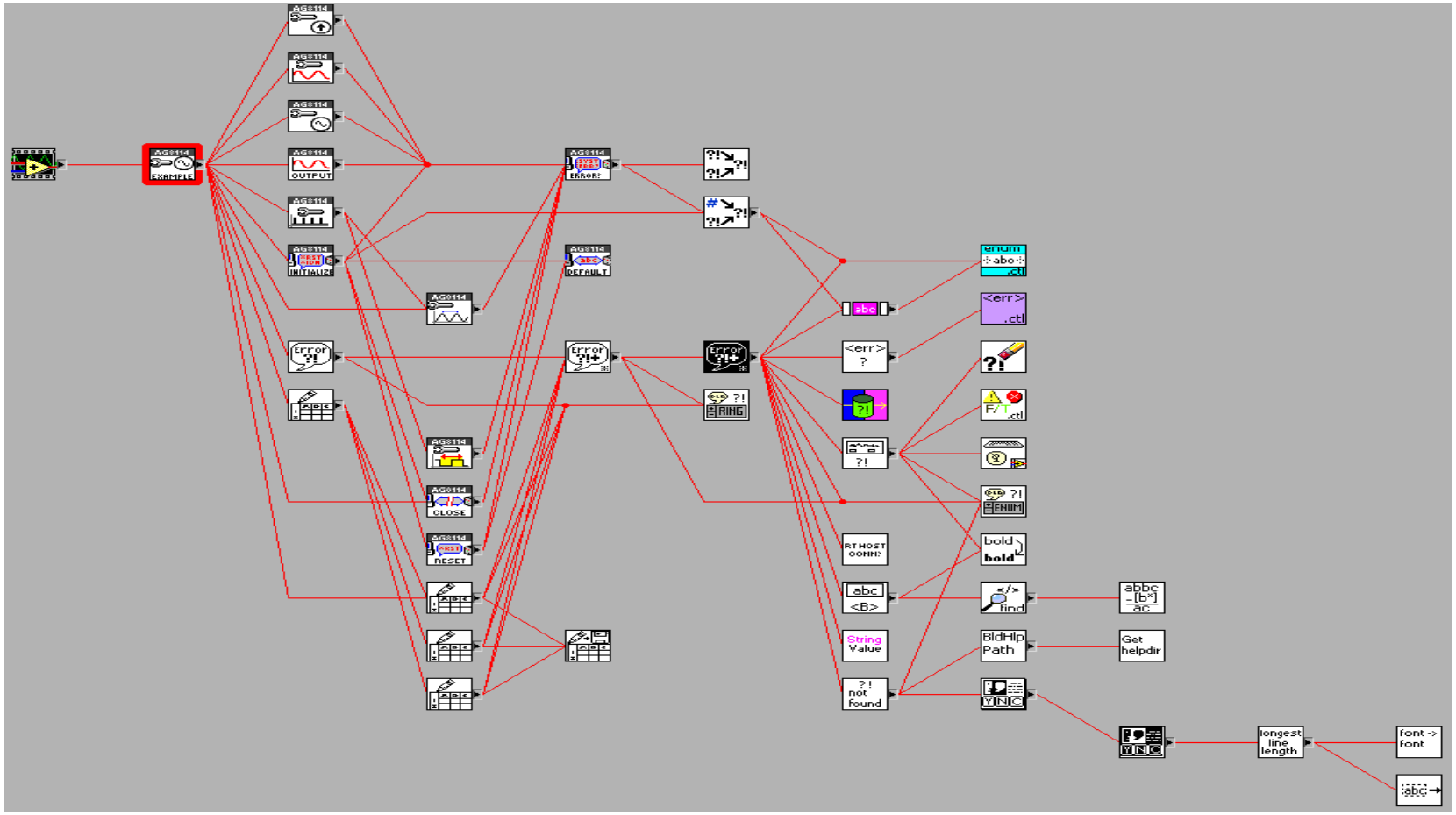

Figure 41. VI Hierarchy for Automated Testing System.

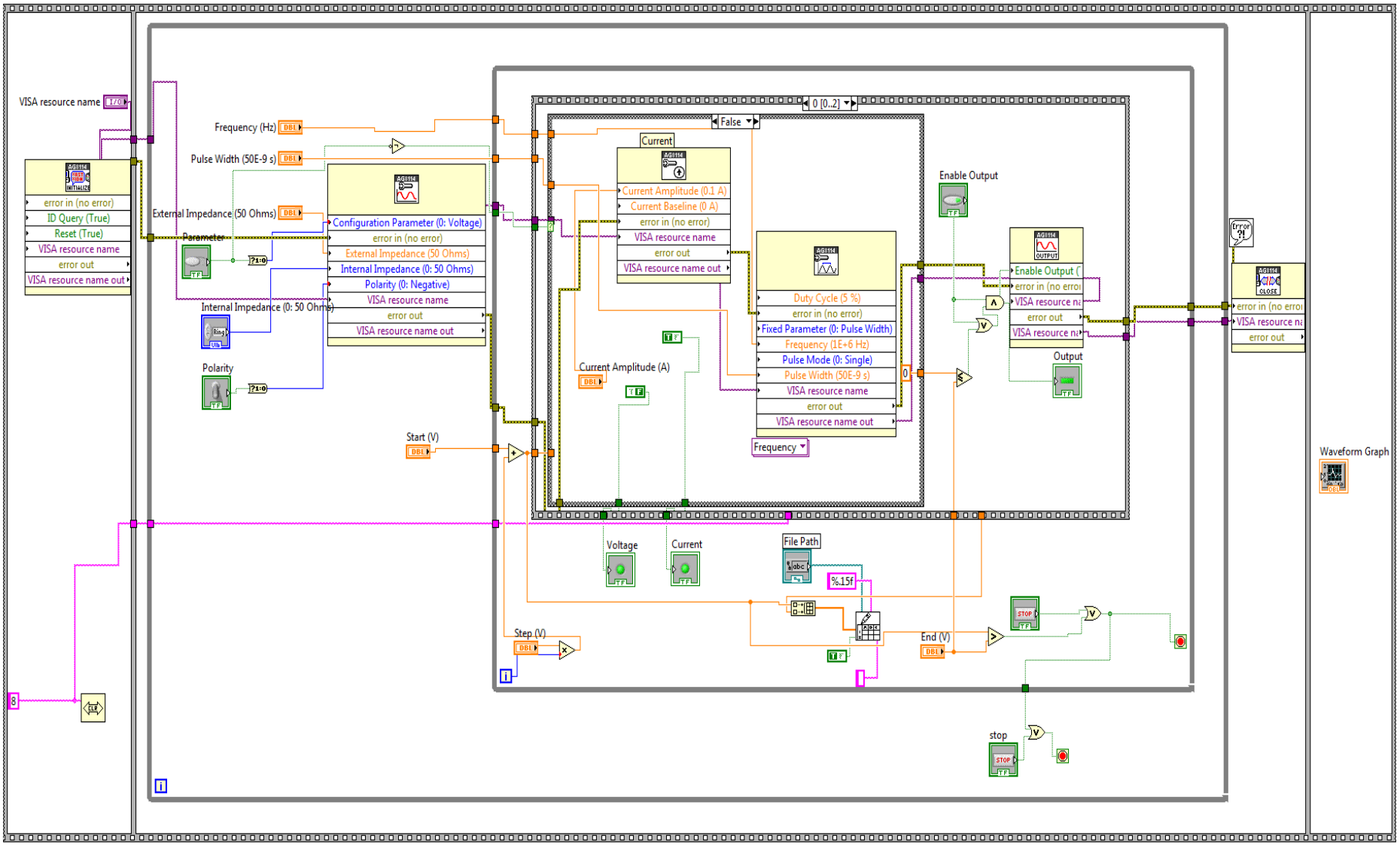

Figure 42. Code sample from Automated Testing System. Not all case states are shown.

Code Examples for Monochromator Control System

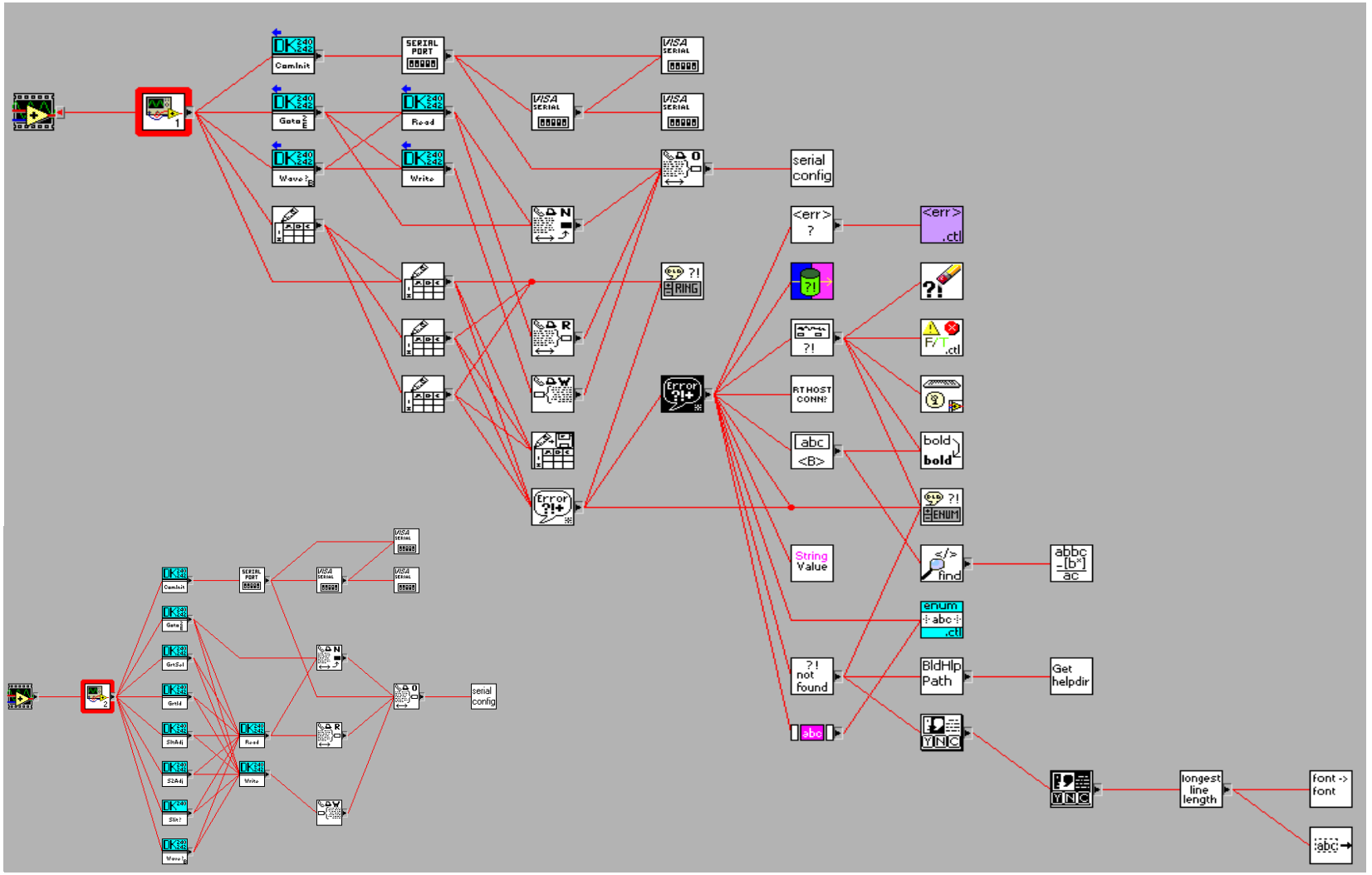

Figure 43. VI Hierarchy for Monochromator Control System.

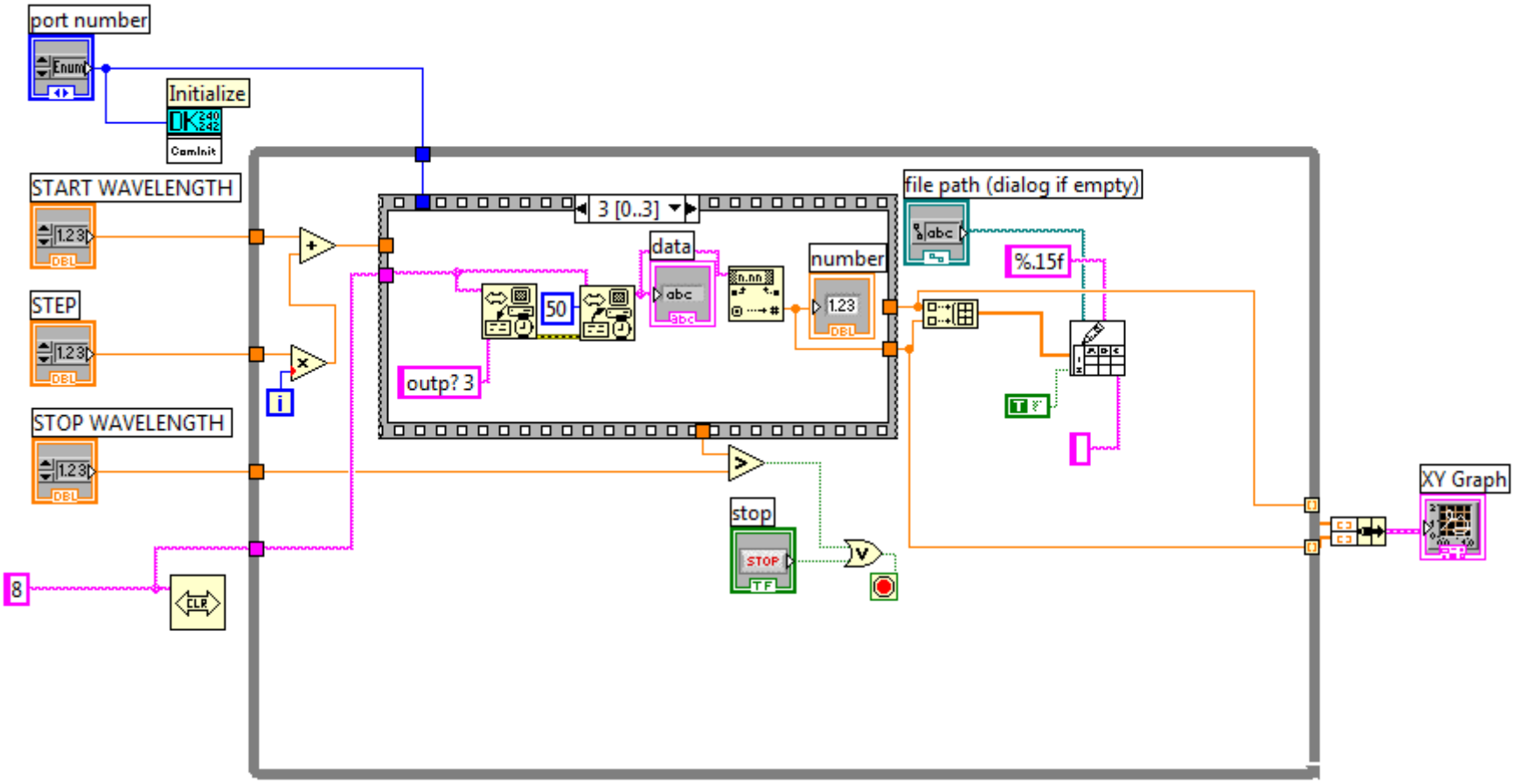

Figure 44. Code sample from Monochromator Control System. Not all case states are shown.

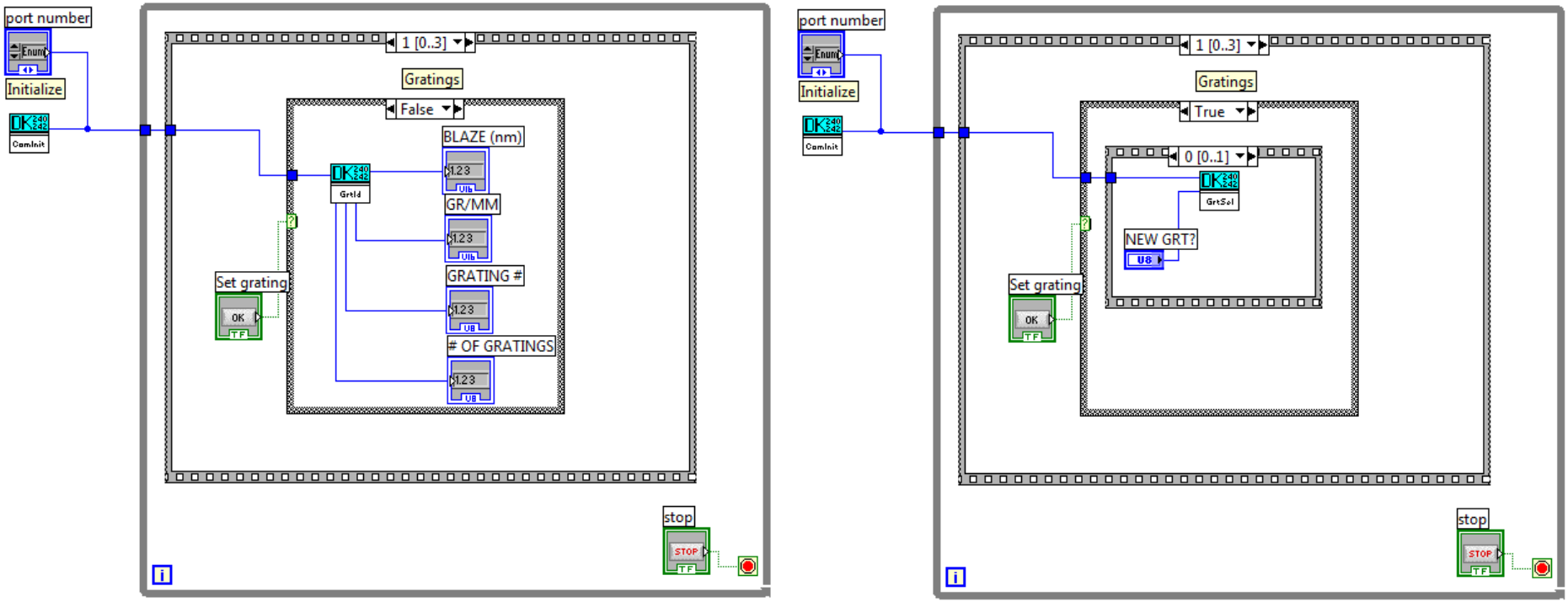

Figure 45. Code sample from Monochromator Control System. Not all case states are shown.